Gravitational lensing constraints on the nature of dark matter

Simona Vegetti - MPA

MPA:
Elisa Ritondale
Francesca Rizzo
Giulia Despali
Wolfgang Enzi

Matt Auger
Oliver Czoske
Chris Fassnacht
John McKean
Carlo Giocoli
Leon Koopmans
Cristiana Spingola
Matus Rybak

Structure formation

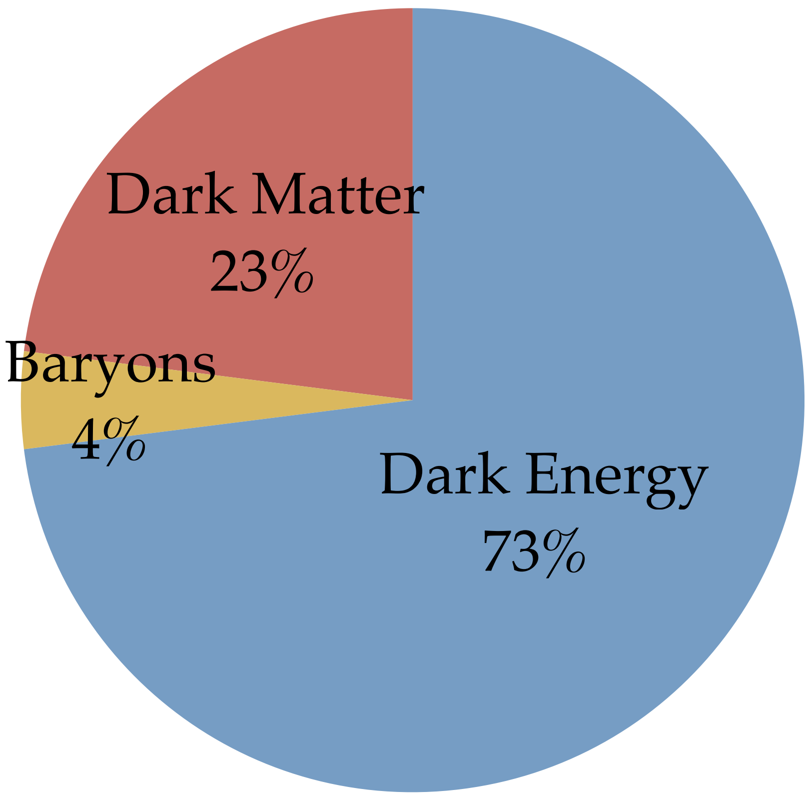

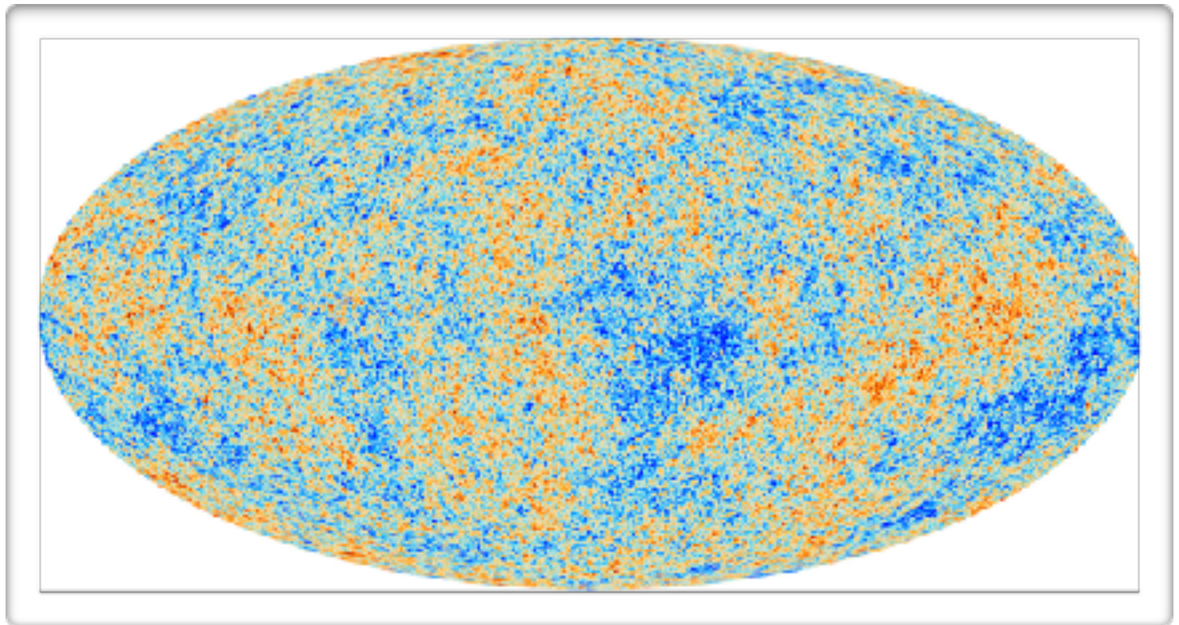

Planck Cosmic Microwave Background

The nature of dark matter shapes the formation of structures in the Universe

Three complementary approaches exist to decipher the nature of dark matter:

- produce DM particles in an accelerator
- direct/indirect detections
- measure the level of clumpiness of the Universe at the smallest scales

Springel+ 2008; Lovell+ 2012

Substructure in the Milky Way Halo

Cold Dark Matter / WIMPs, Axions

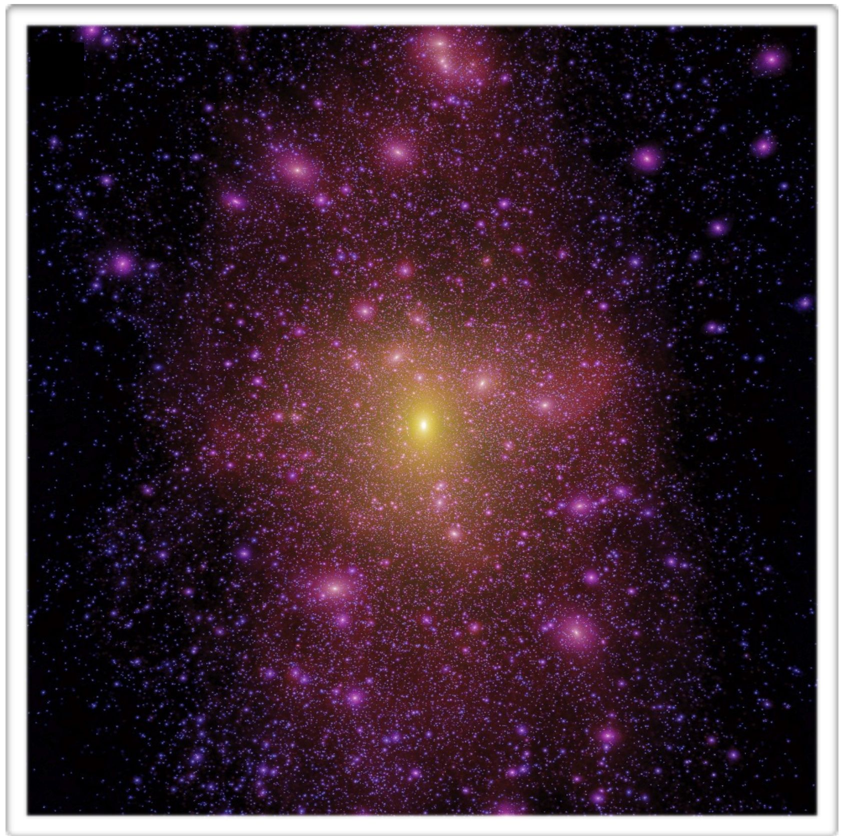

Warm Dark Matter / e.g. sterile neutrinos

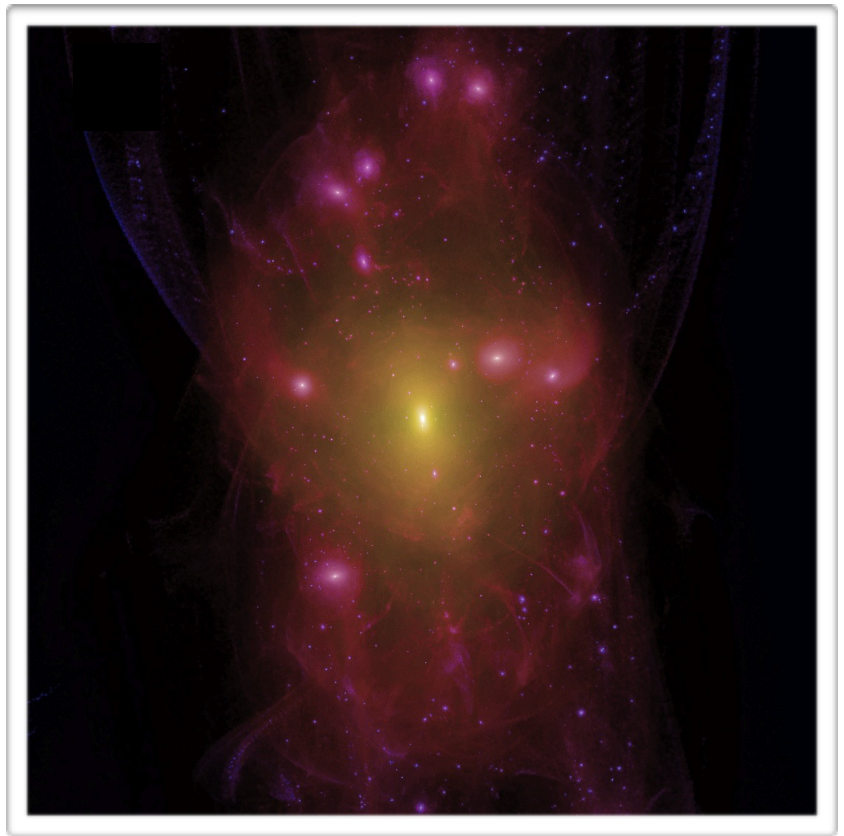

The total number of substructure strongly depends on the nature of dark matter

Substructure in the Milky Way Halo

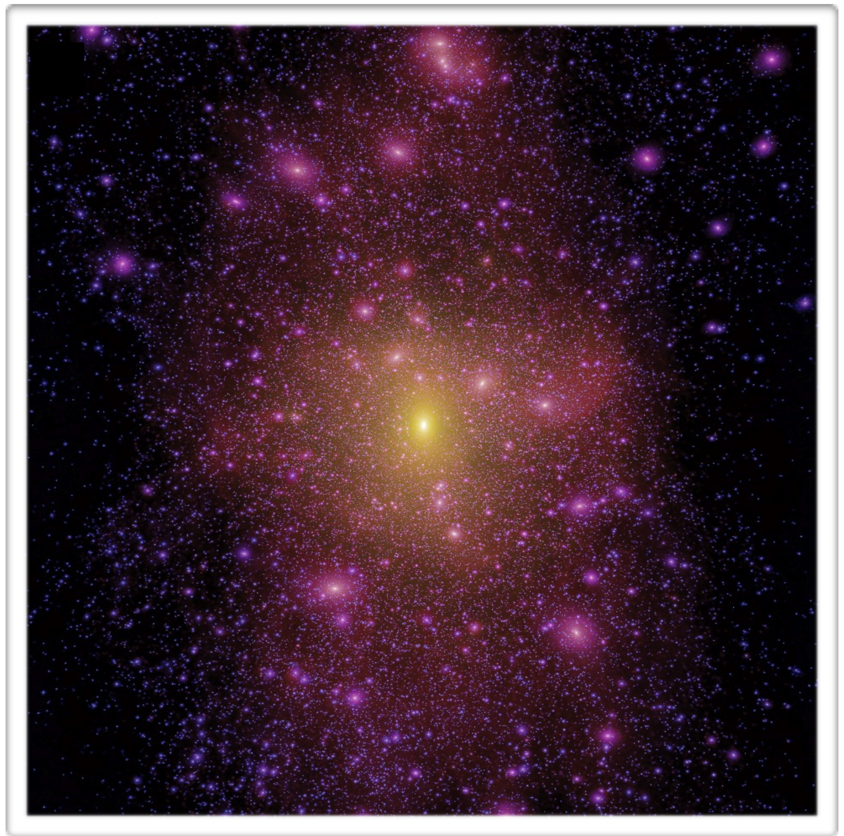

Cold Dark Matter

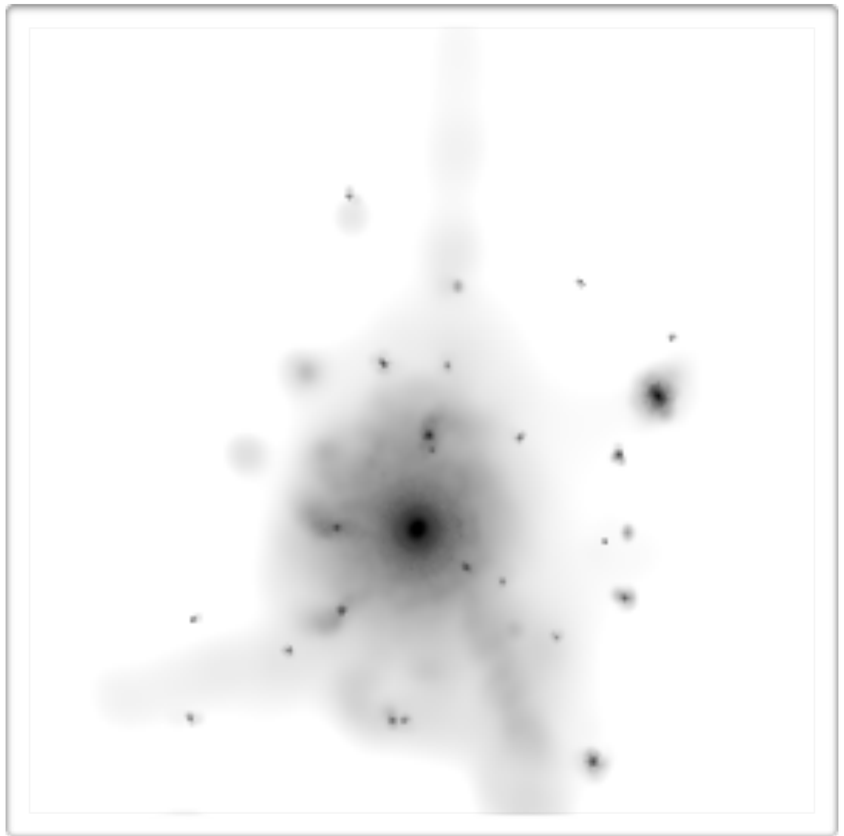

CDM - Stars

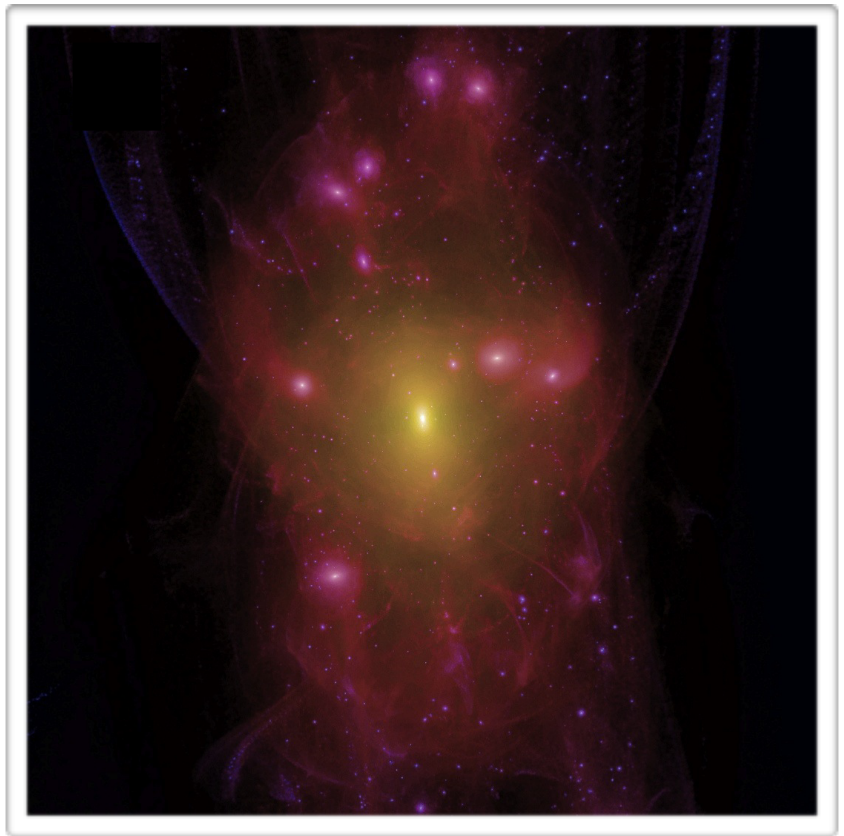

Warm Dark Matter

- There is a degeneracy in the number of observable substructures between dark and galaxy formation models
- Most of the low mass substructure are dark

Substructure mass function

Predicted abundance of substructure in the Milky Way halo

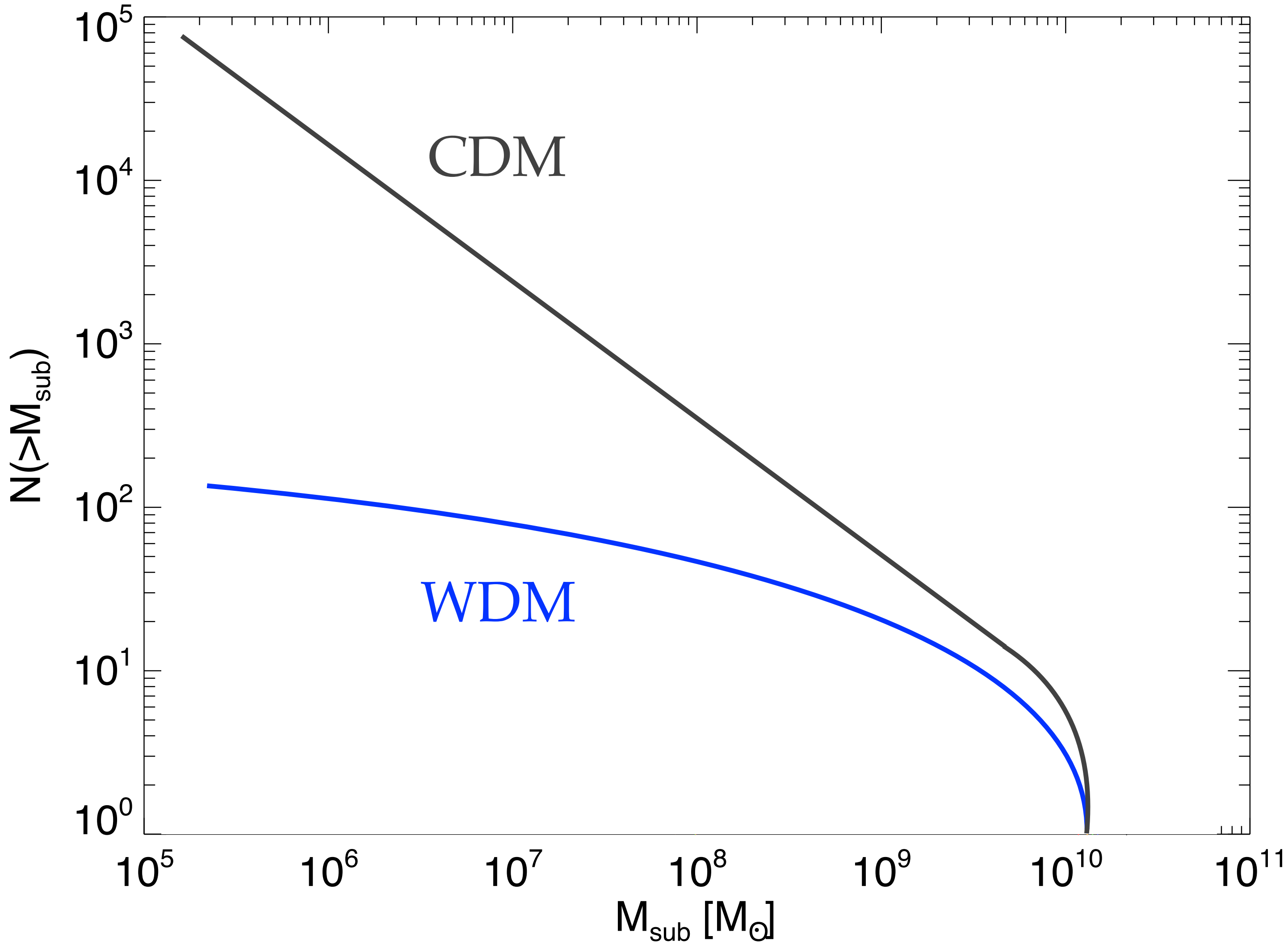

$$P_{\rm WDM}(k) = T^2(k) P_{\rm CDM}(k)$$

$$T(k) = (1 + (\alpha k)^{2\nu})^{-5/\nu}$$

CDM

$$dN/dM \propto f M^{-\alpha}$$

WDM models

$$dN/dM \propto f M^{-\alpha} (1 + M_c/M)^{\beta}$$

Gravitational Lensing

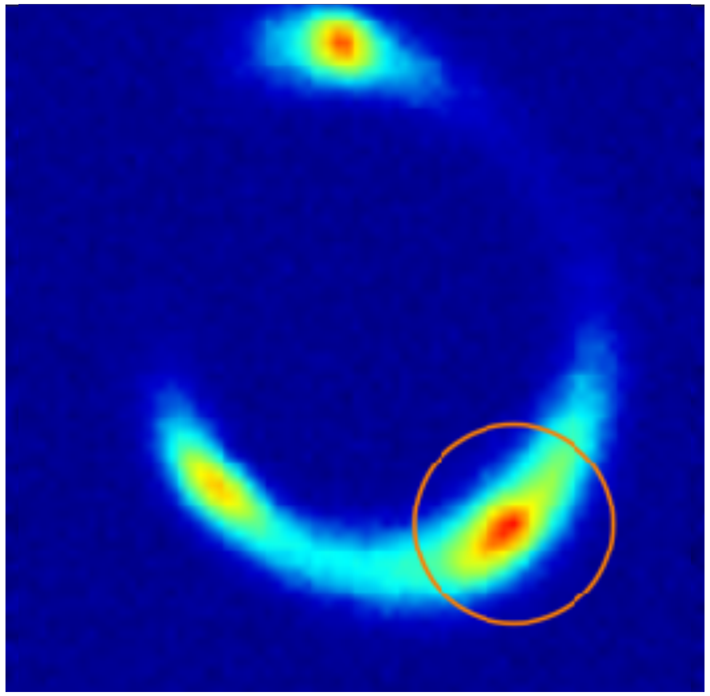

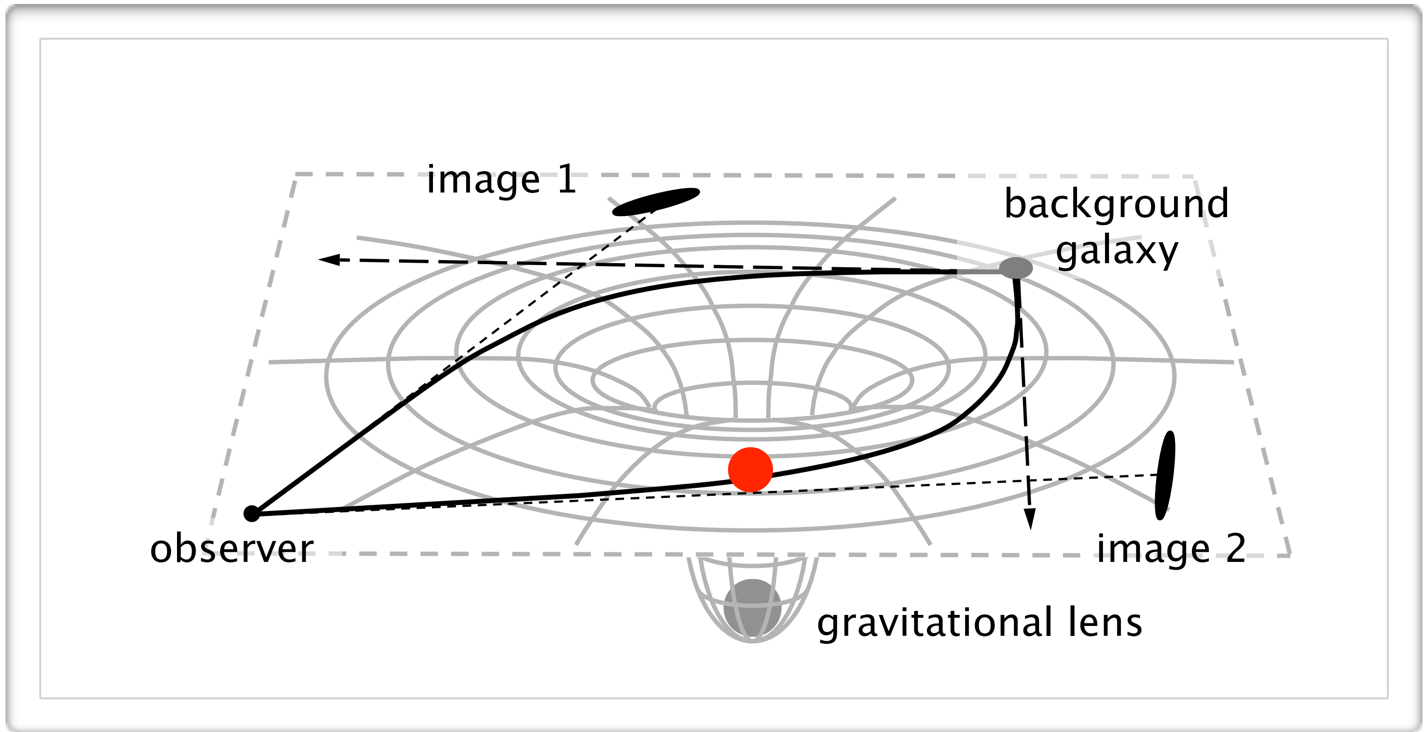

Vegetti & Koopmans, 2009   Ritondale+ 2017

Gravitational Imaging

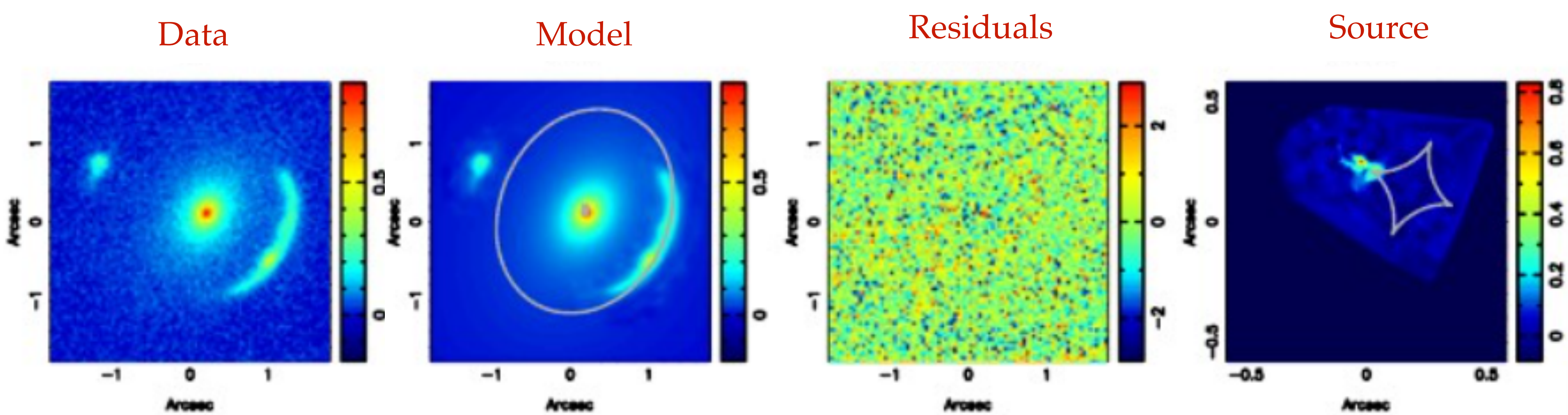

Smooth analytic power-law model $\psi(\mathbf{x}, \eta)$

Sersic profile $\Sigma(\mathbf{x}, \eta')$

Pixellated regularized source

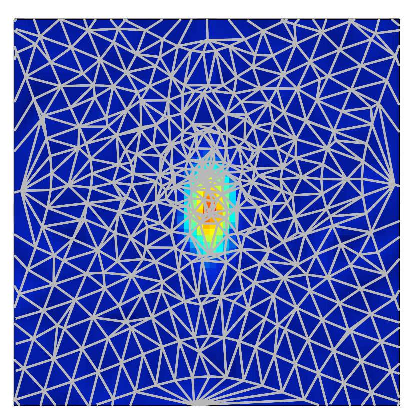

$$P = \chi^2 + \lambda_s^2\ \mathbf{H^T H s}$$

Gravitational Imaging

Data Model Residuals Source

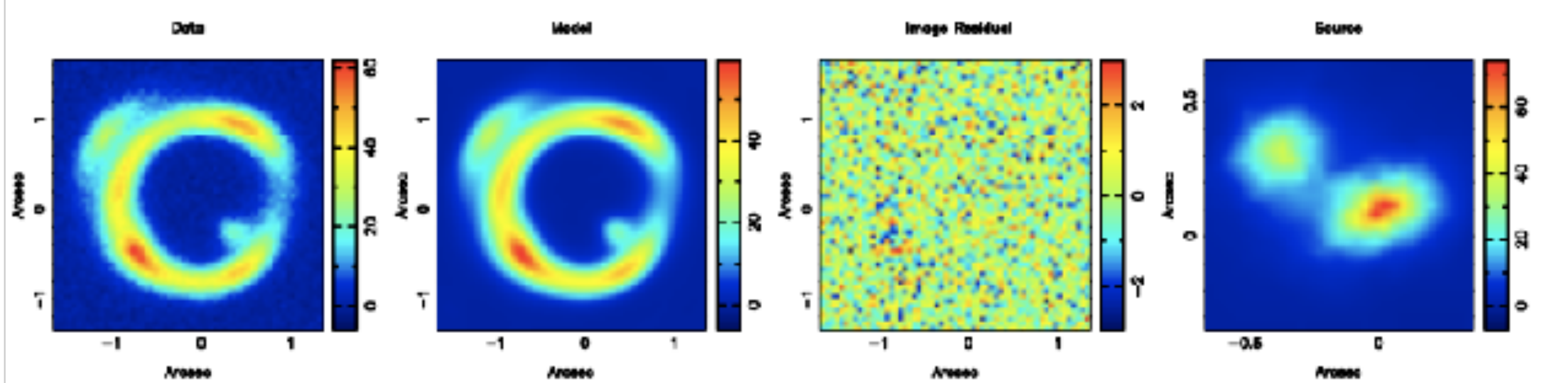

$$\psi(\mathbf{x},\eta)_{tot} = \psi(\mathbf{x},\eta) + \delta\psi(\mathbf{x})$$

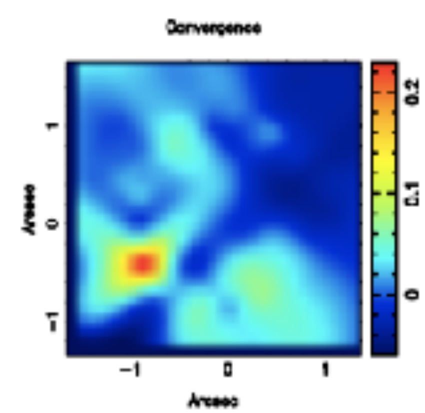

Density corrections

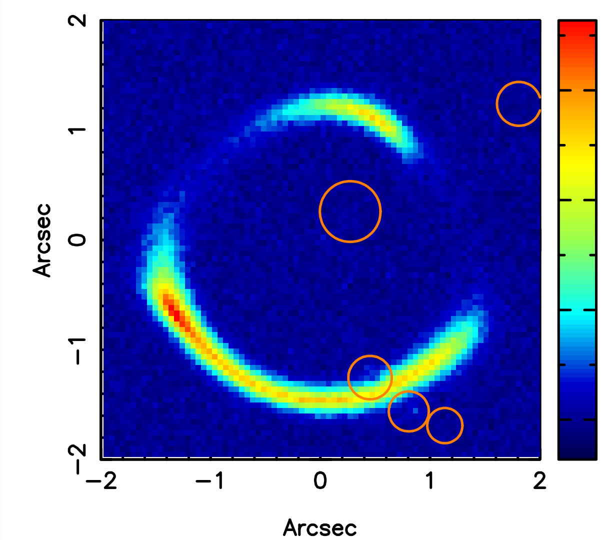

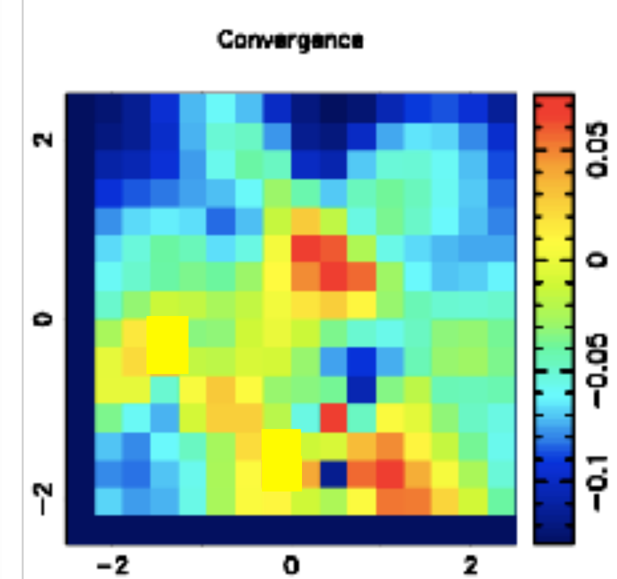

- Substructures are detected as corrections to an overall smooth potential
- If present, more than one substructure can be detected and quantified

Criteria for detection

- a positive convergence correction that improves the image residuals is found independently from the potential regularization, number of source pixels, PSF rotations, and galaxy subtraction procedure;

- the mass and the position of the substructure obtained via the posterior exploration is consistent with those independently obtained by the potential corrections and the MAP parametric clumpy model;

- a clumpy model is preferred over a smooth model with a Bayes factor $\Delta \log E = \log E_{smooth} - \log E_{clumpy} >= -50$ (to first order equivalent to a 10-σ detection, under the assumption of Gaussian noise);

- the results are consistent among the different filters, where available.

Why not blobolgy?

Methods based on analytic descriptions of single mass clumps can lead to false detections

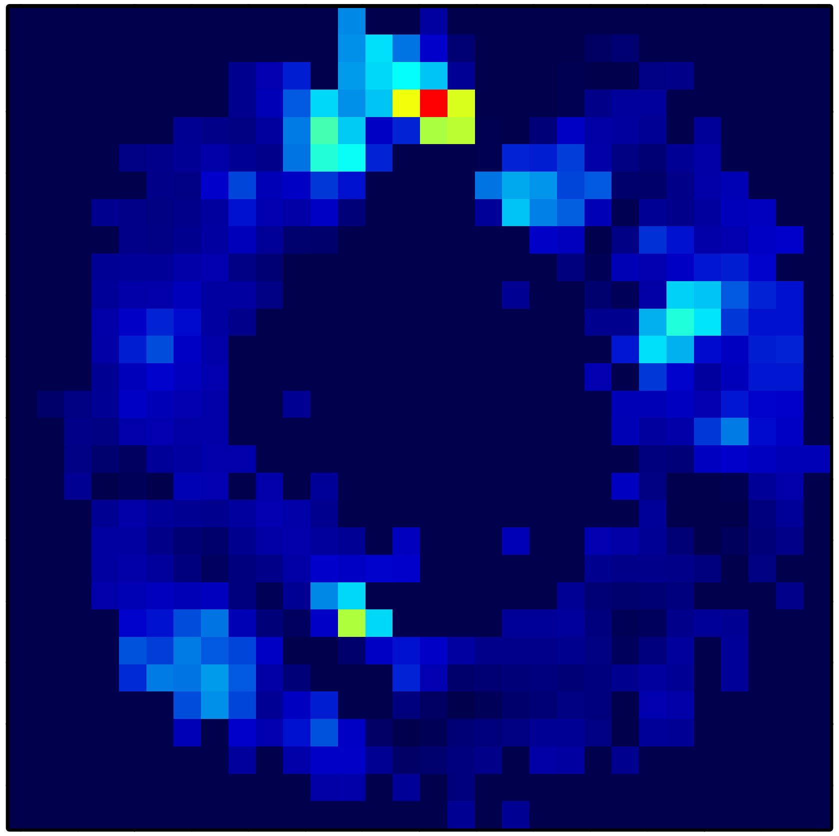

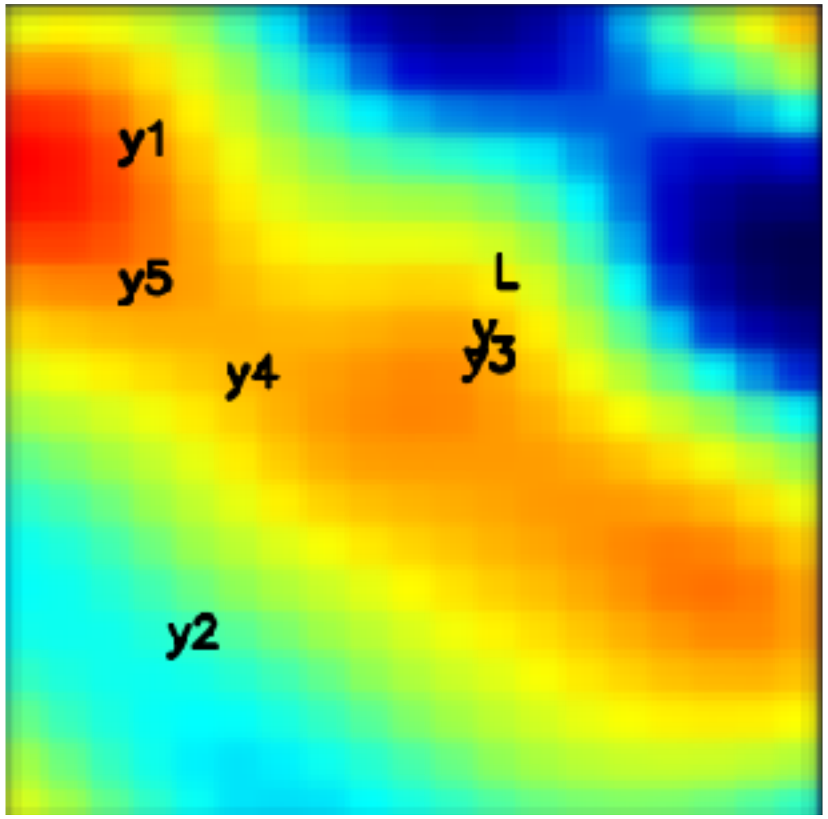

ΔLogE=1130 (47 sigma)

ΔlogE=1388 (52 sigma)

ΔlogE=1536 (55 sigma)

Substructure Sensitivity

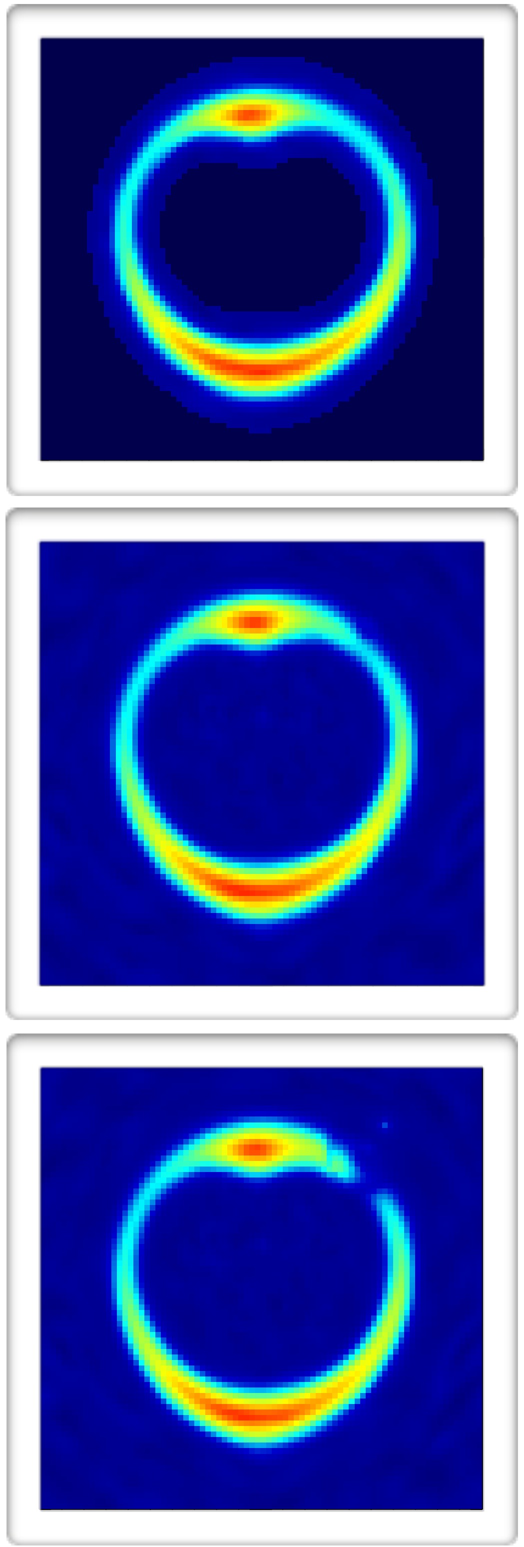

Increasing mass

Rau, Vegetti & White 2013, MNRAS

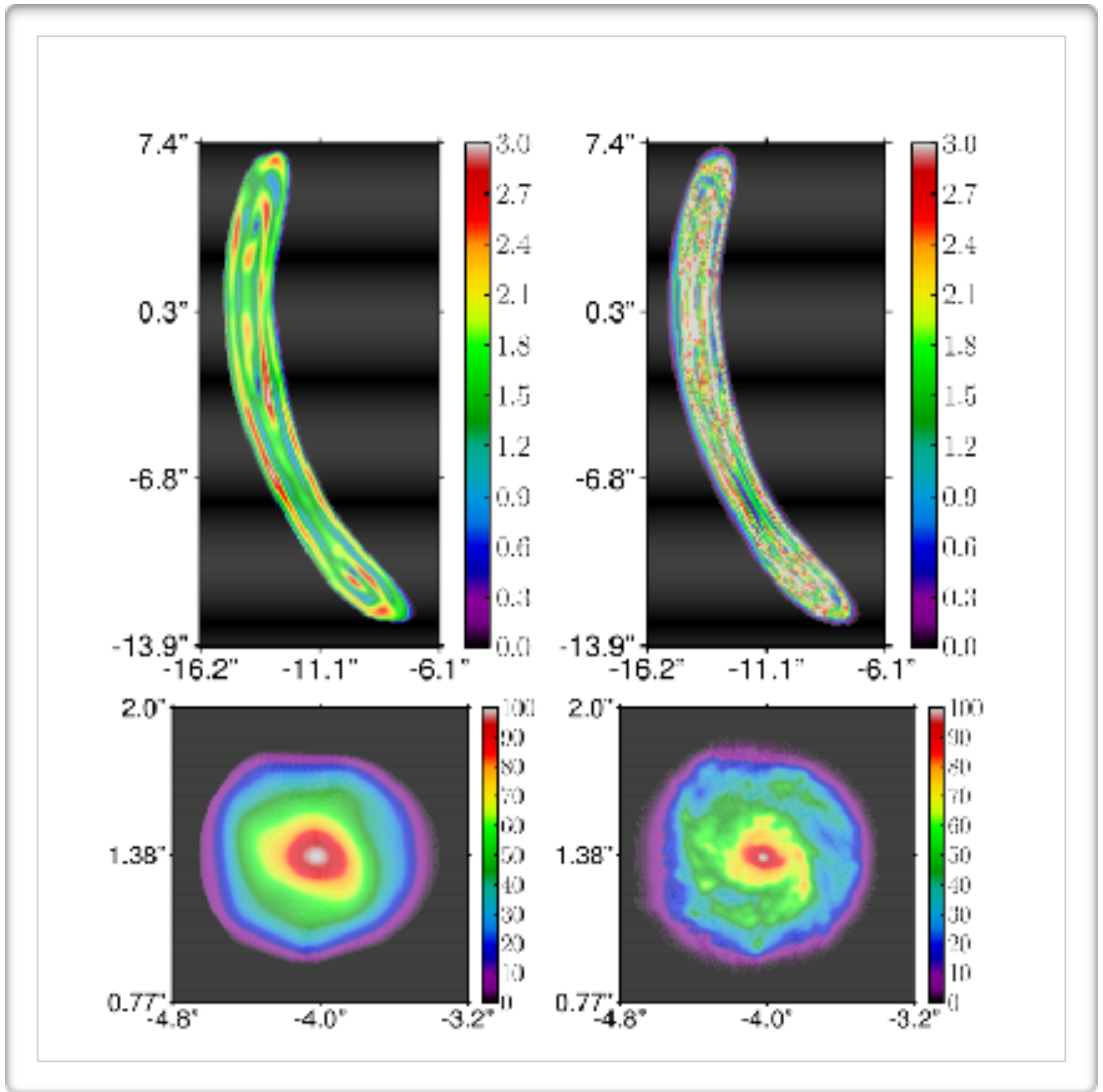

Increasing level of source complexity

Predictions

Substructure mass function

Predicted abundance of substructure in the Milky Way halo

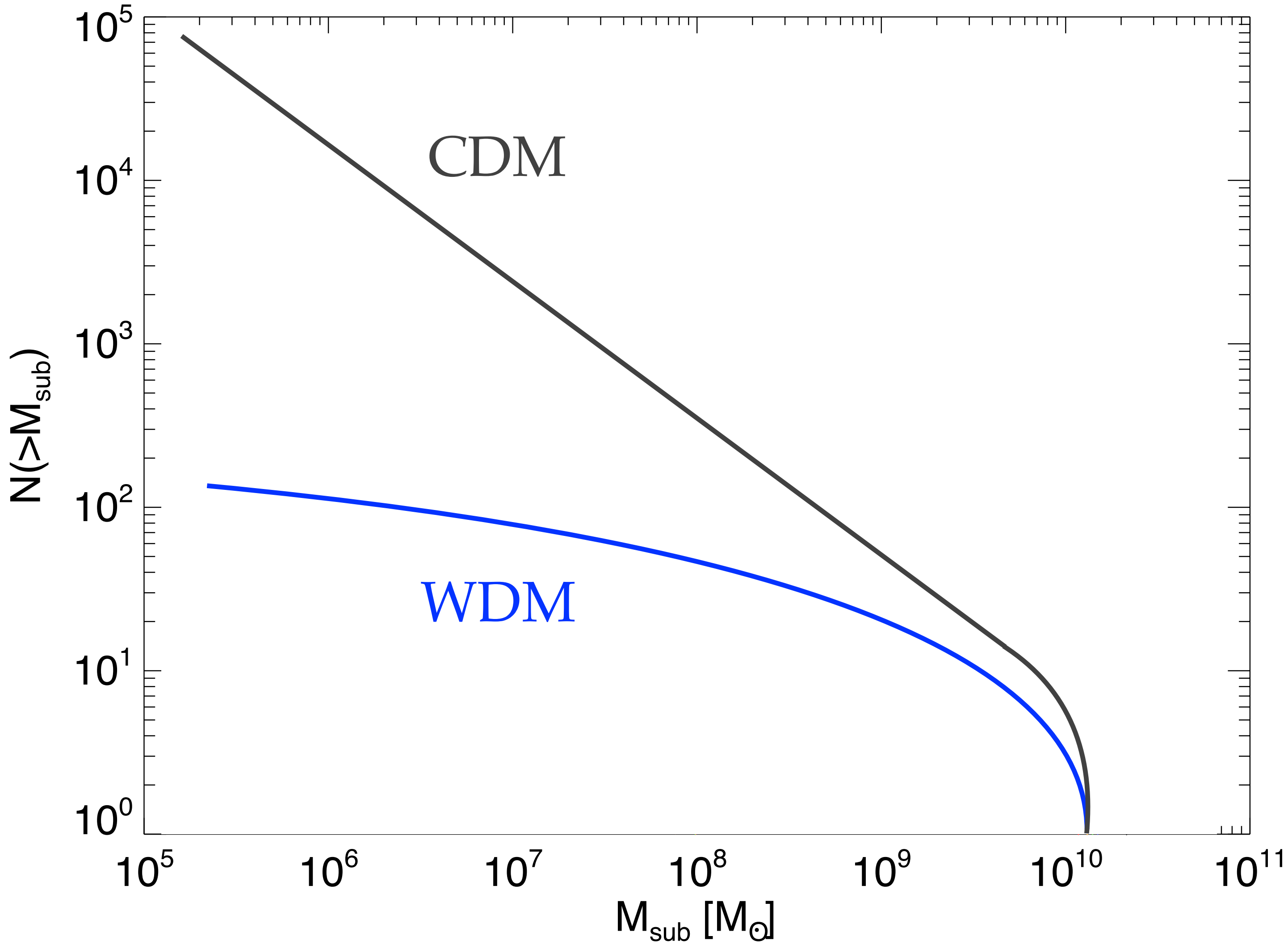

$$P_{\rm WDM}(k) = T^2(k) P_{\rm CDM}(k)$$

$$T(k) = (1 + (\alpha k)^{2\nu})^{-5/\nu}$$

CDM

$$dN/dM \propto f M^{-\alpha}$$

WDM models

$$dN/dM \propto f M^{-\alpha} (1 + M_c/M)^{\beta}$$

Predictions

Open questions:

- What are the correct predictions for gravitational lensing?
- What is the effect of baryons? And is there a on the SBHMF degeneracy between DM and galaxy formations models?
- What are the predictions for DM models beyond CDM & WDM?
- What is the contribution of small-mass haloes along the line-of-sight?

Vogelberger+2014; Shaye+ 2015

Eagle & Illustris

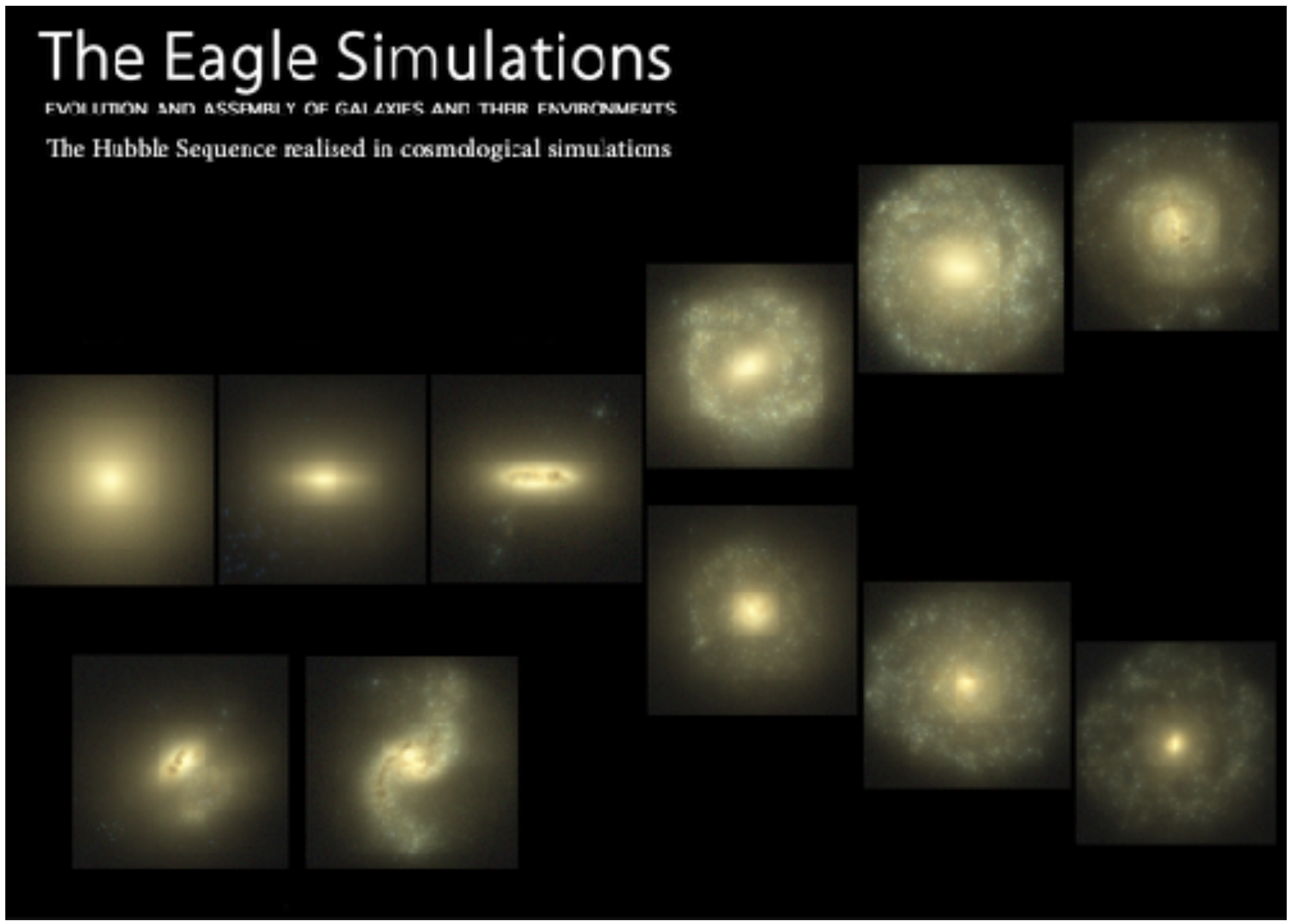

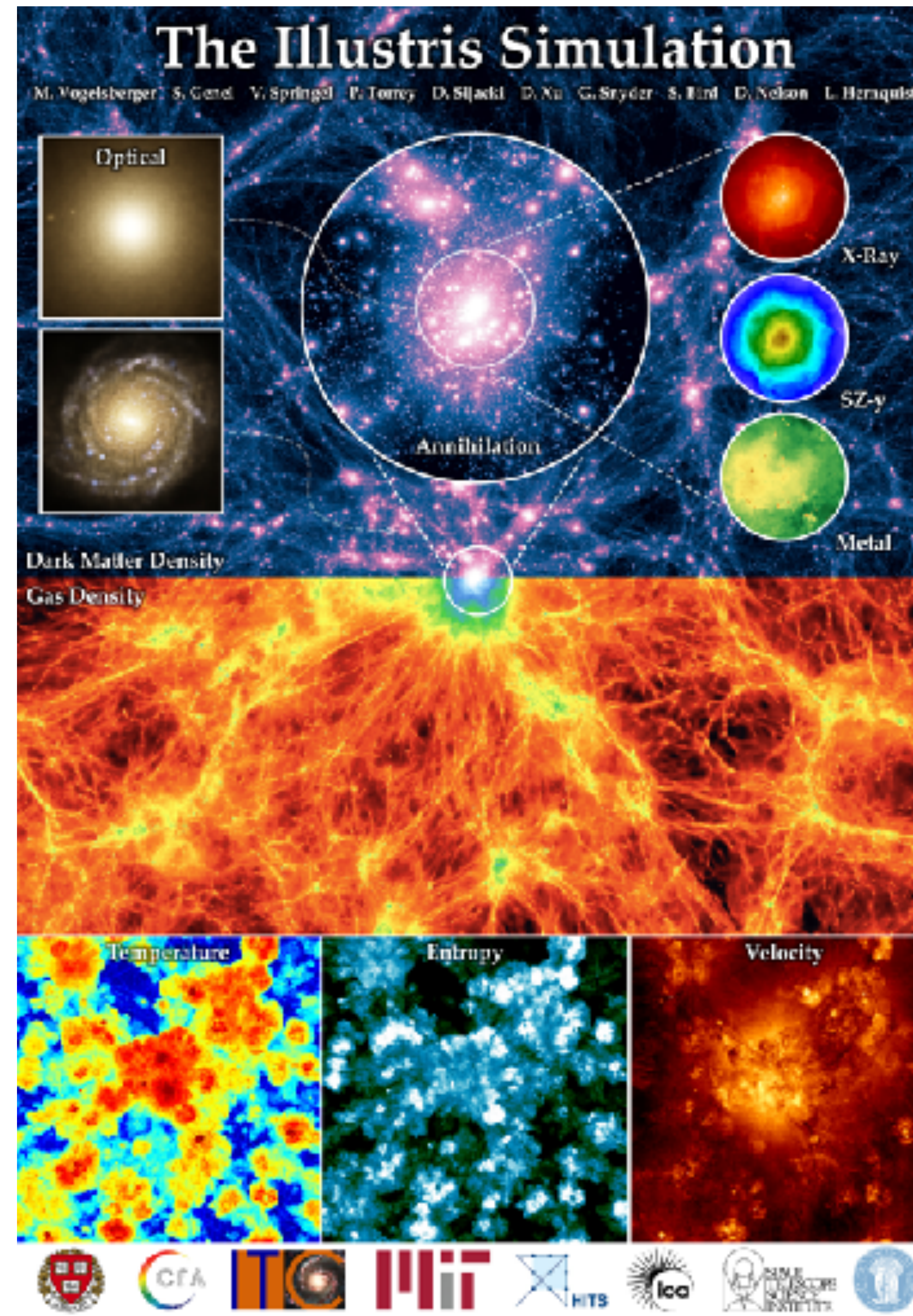

name	volume [(Mpc)^3]	DM particles / hydro cells / MC tracers	$\epsilon_{baryon}/\epsilon_{DM}$ [pc]	m_{baryon}/m_{DM} [10^5 M$_\odot$]	r_{cell}^{min} [pc]
Illustris-1	106.5^3	$3 \times 1,820^3 \cong 18.1 \times 10^9$	$710/1,420$	$12.6/62.6$	48
Illustris-2	106.5^3	$3 \times 910^3 \cong 2.3 \times 10^9$	$1,420/2,840$	$100.7/501.0$	98
Illustris-3	106.5^3	$3 \times 455^3 \cong 0.3 \times 10^9$	$2,840/5,680$	$805.2/4008.2$	273
Illustris-Dark-1	106.5^3	$1 \times 1,820^3$	$710/1,420$	$-/75.2$	–
Illustris-Dark-2	106.5^3	1×910^3	$1,420/2,840$	$-/601.7$	–
Illustris-Dark-3	106.5^3	1×455^3	$2,840/5,680$	$-/4813.3$	–

Lens Analogues

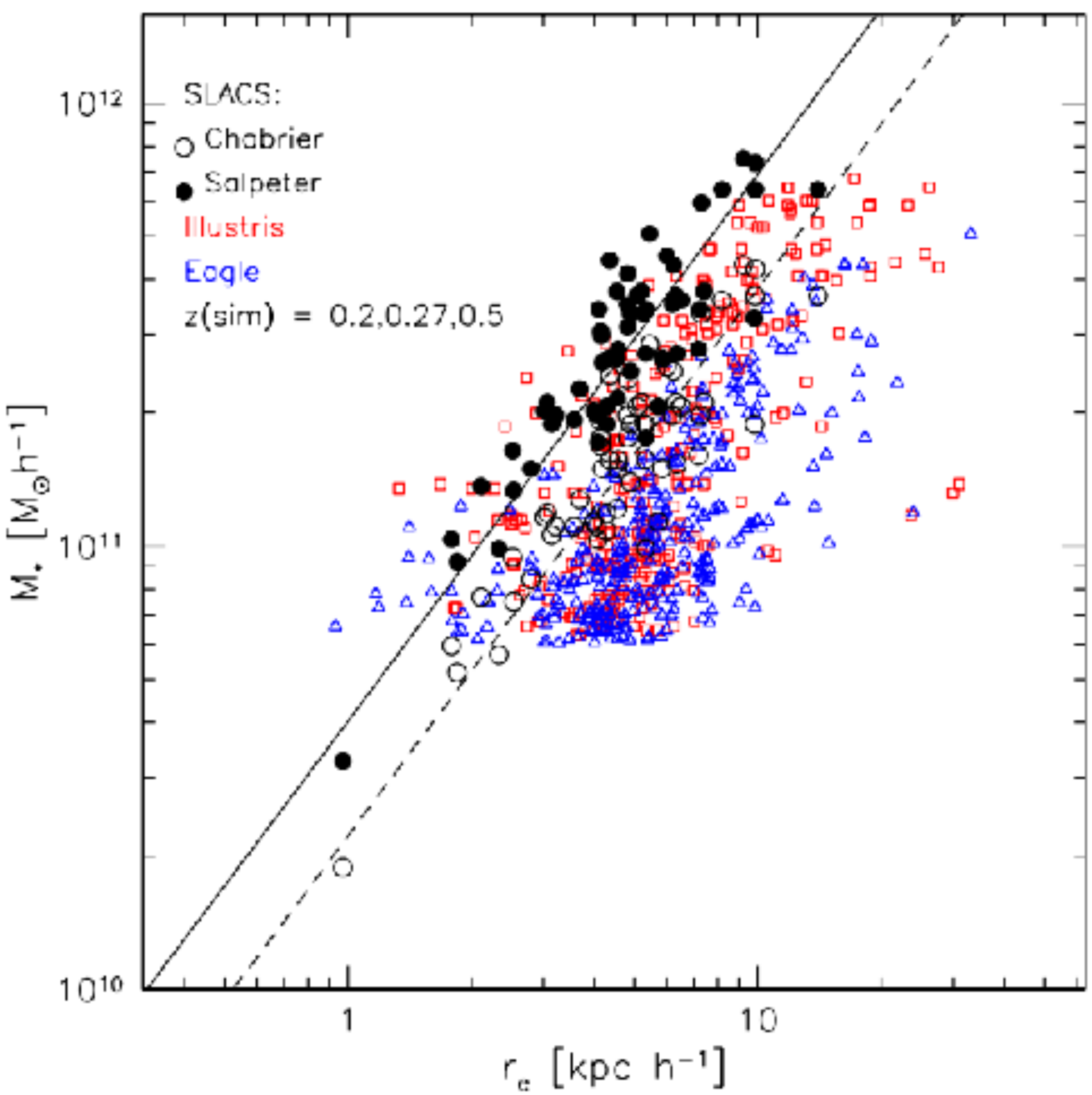

SLACS: Early-Type galaxies with:

$$M_* = 10^{10.5} - 10^{11.8} M_\odot$$

$$z \sim 0.06 - 0.3$$

SLACS analogues:

Relaxed haloes with matching velocity dispersion and z range

Dynamically selected to be Early-Type

With total stellar mass and effective radius consistent with the SLACS lenses

SHMF: the role of baryons

Different HMF propagate into different subhalo mass function with depletion at the low-mass end

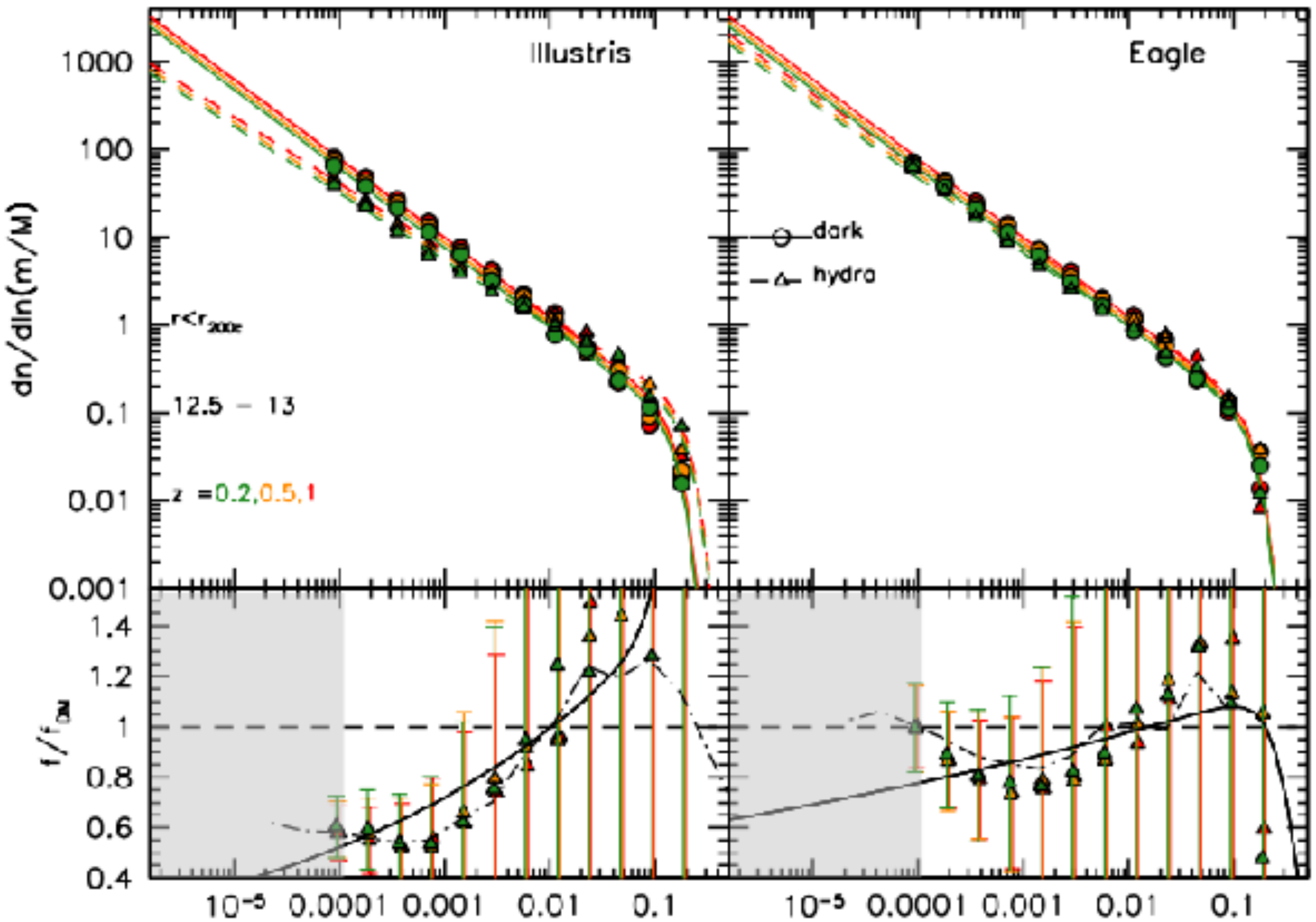

EAGLE: 20 % fewer sub-haloes between 10^8 and 10^9 M_{sun}
Illustris: 40% fewer

There is an increase in the amount of substructure with host halo mass and redshift

A key parameter is

the host halo ellipticity

SHMF: the role of baryons

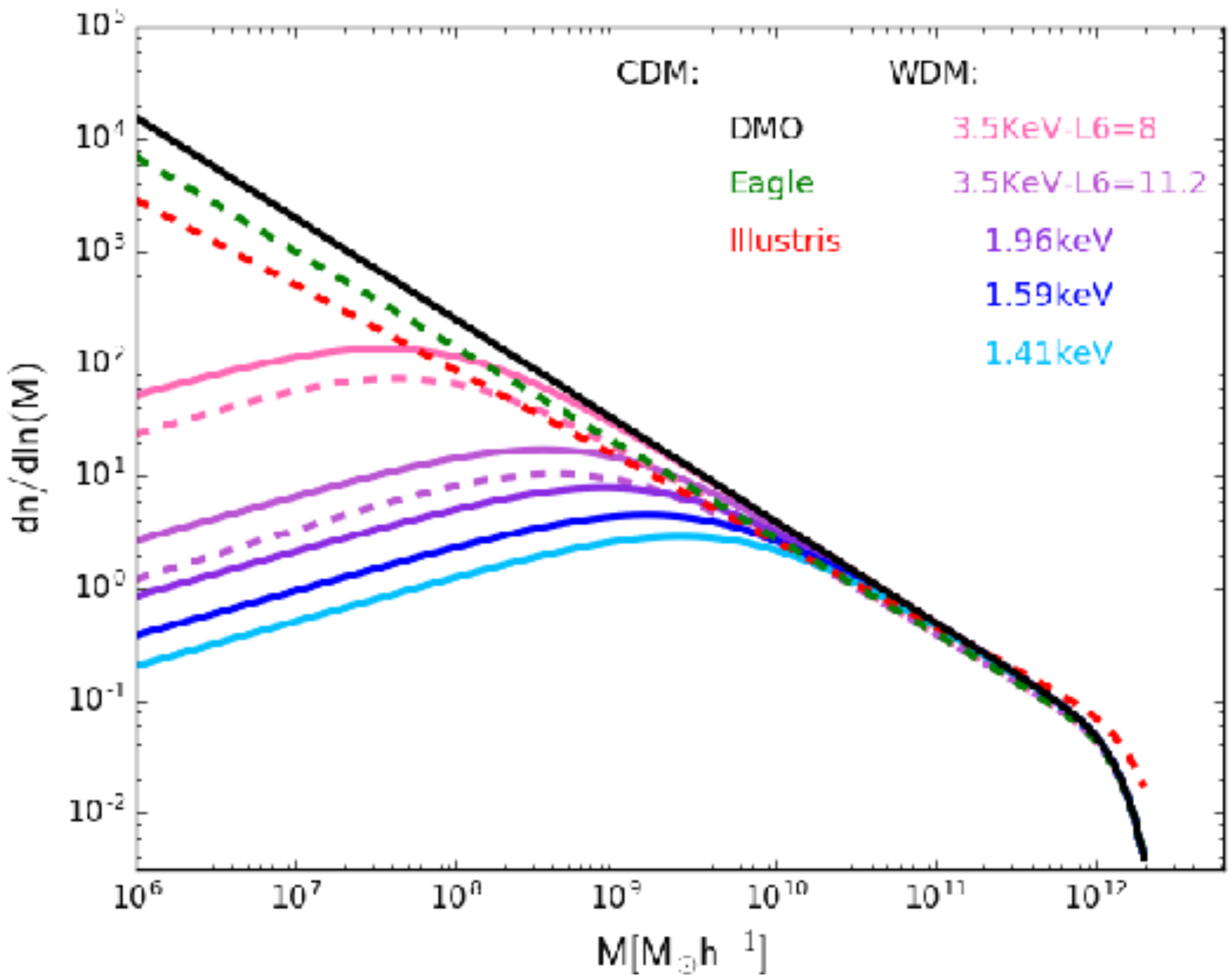

To obtain a more complete set of predictions we need to investigate a larger number of DM and galaxy formation models

Despali et al. in prep.

SIDM

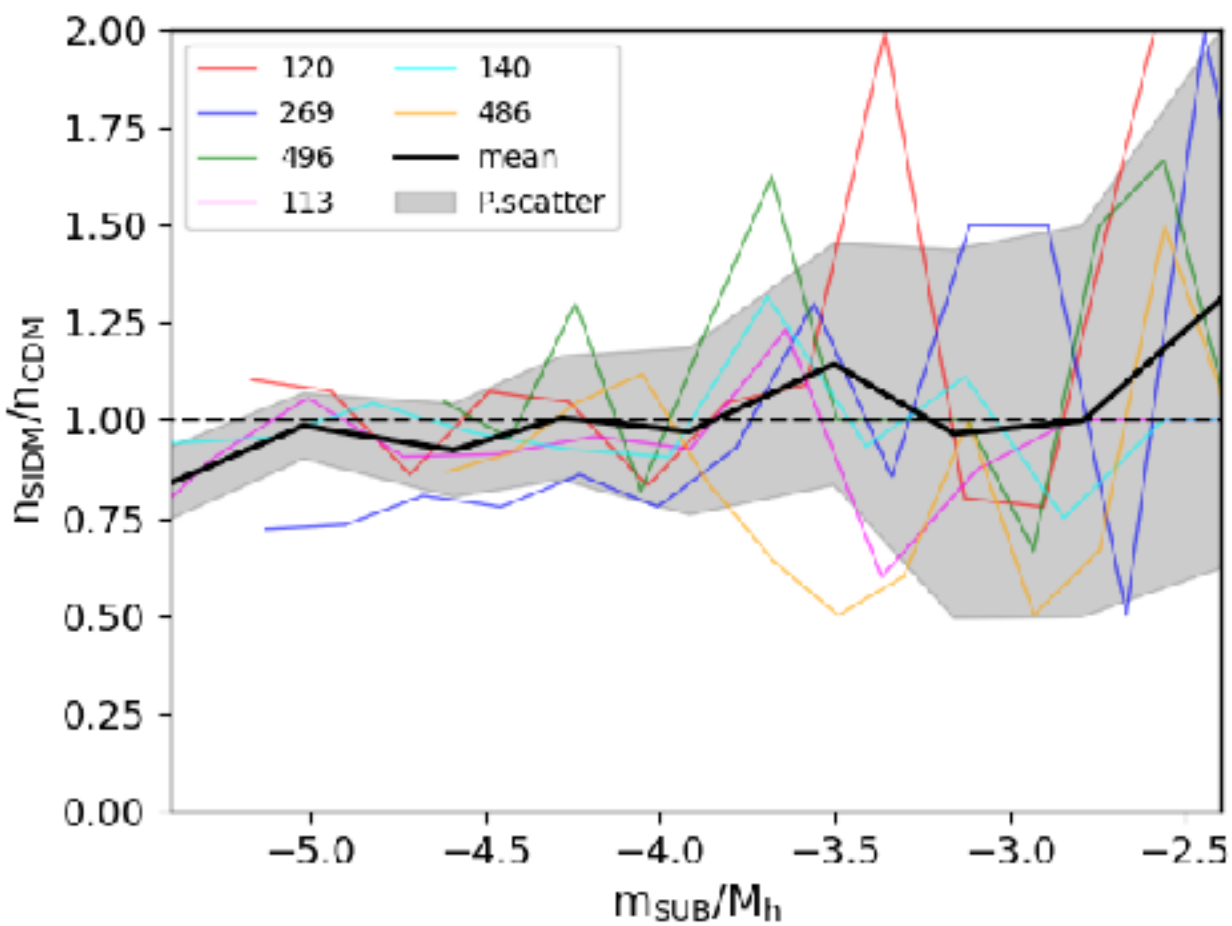

- the number of subhaloes tends to be a bit lower at low masses in SIDM, but not by much

in most cases the central density is lower in the SIDM and the stars effective radius is larger

- profiles differs within the few central kpc and thus they create smaller Einstein rings

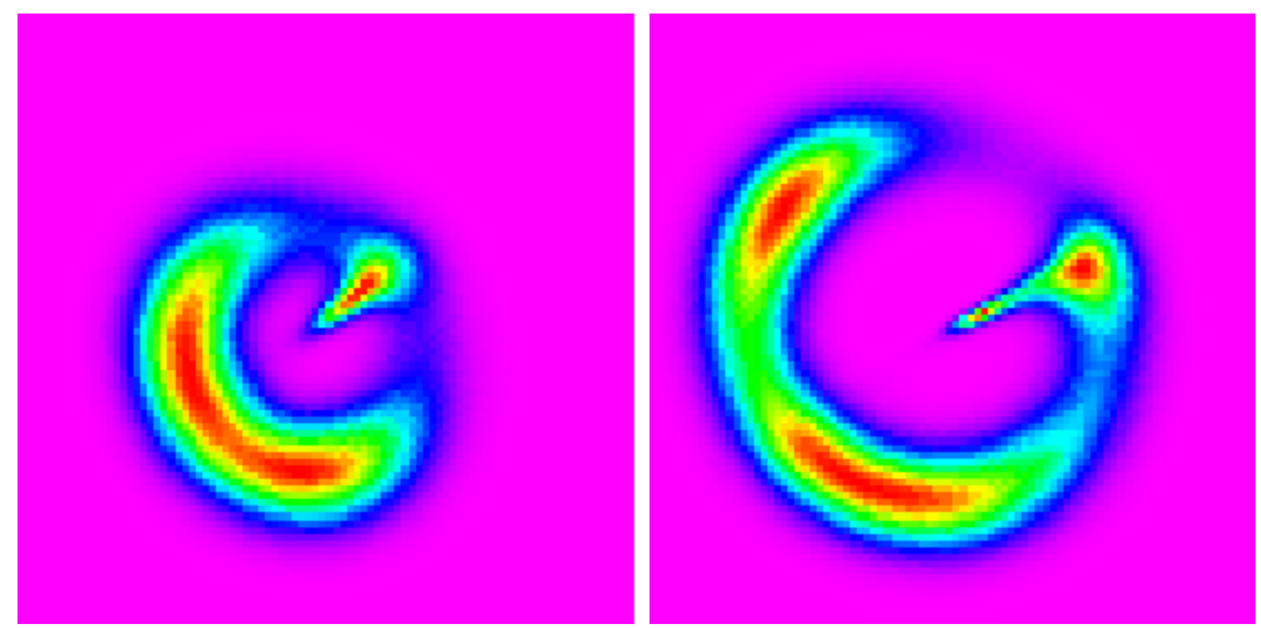

- some of them would not be classified as SLACS analogues anymore

LOS contribution

Gravitational lensing is sensitive not only to the mass distribution on the lensing galaxy but also to the general mass distribution along the line-of-sight

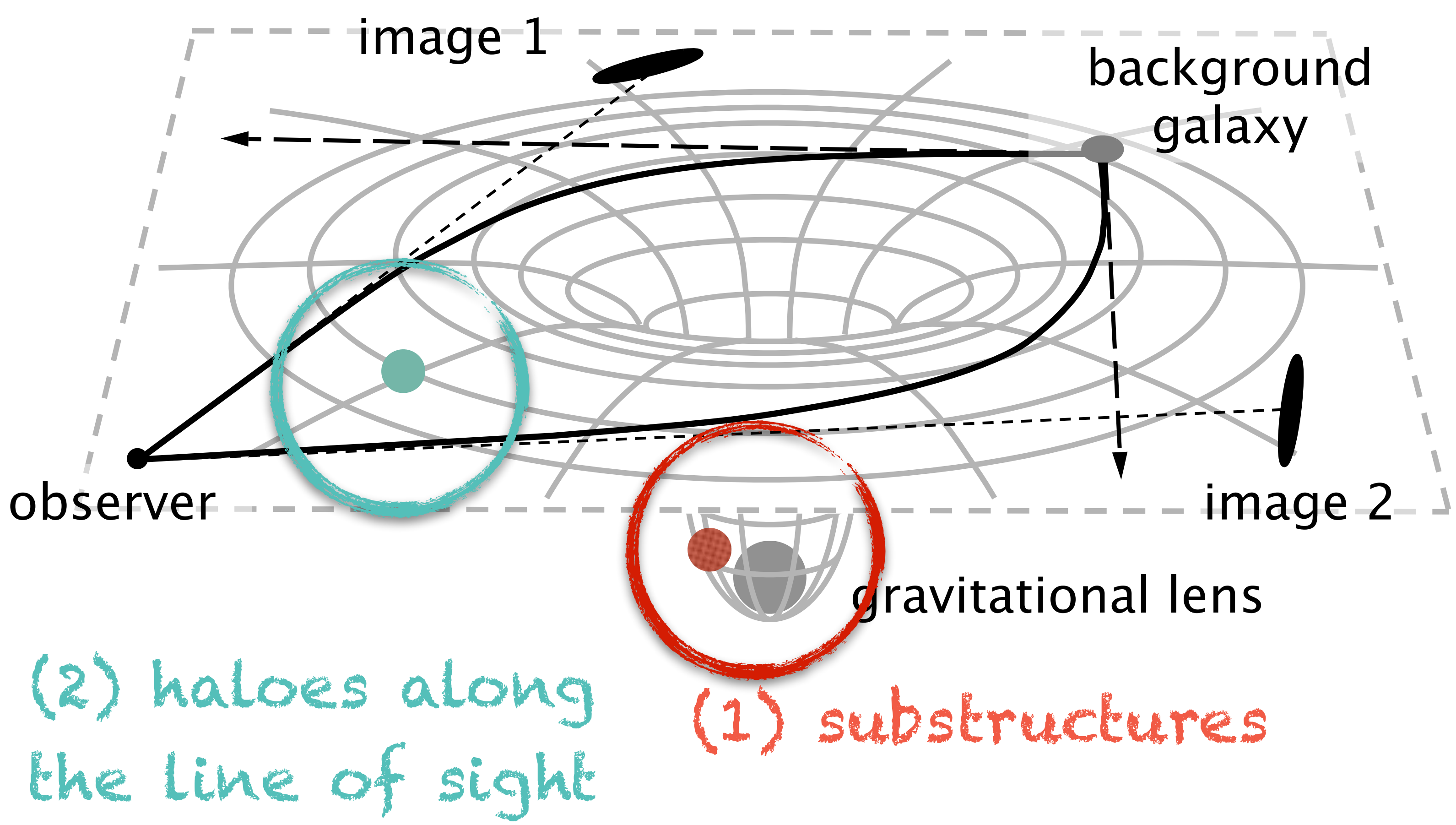

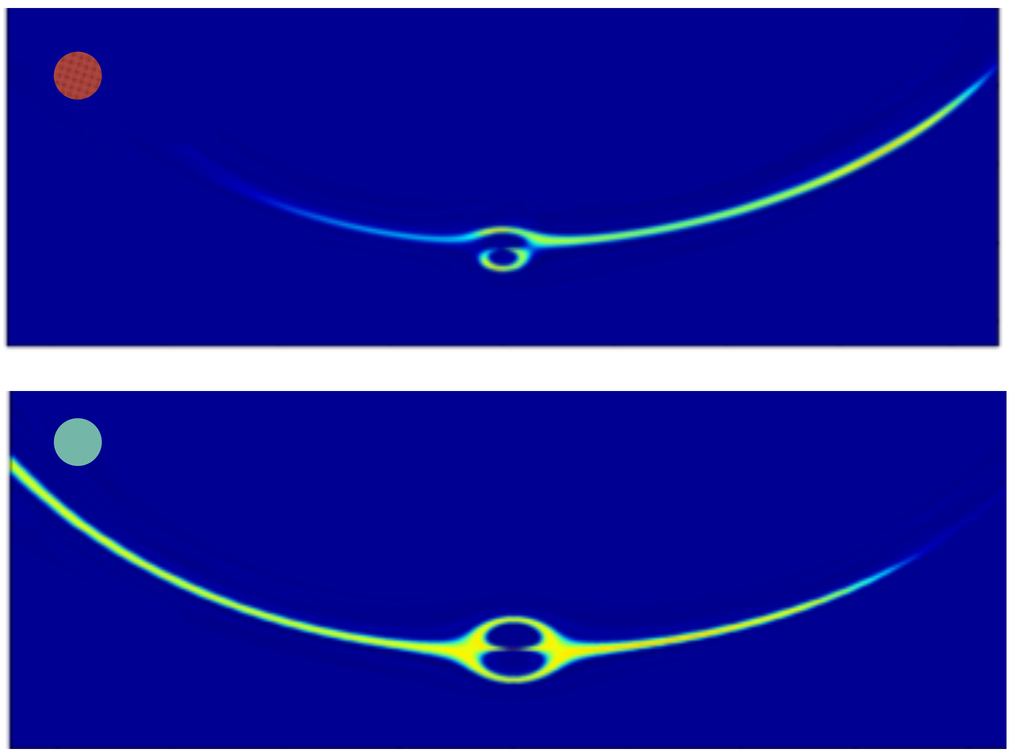

LOS is not a contamination but a powerful and clean probe on the nature of DM

LOS contribution

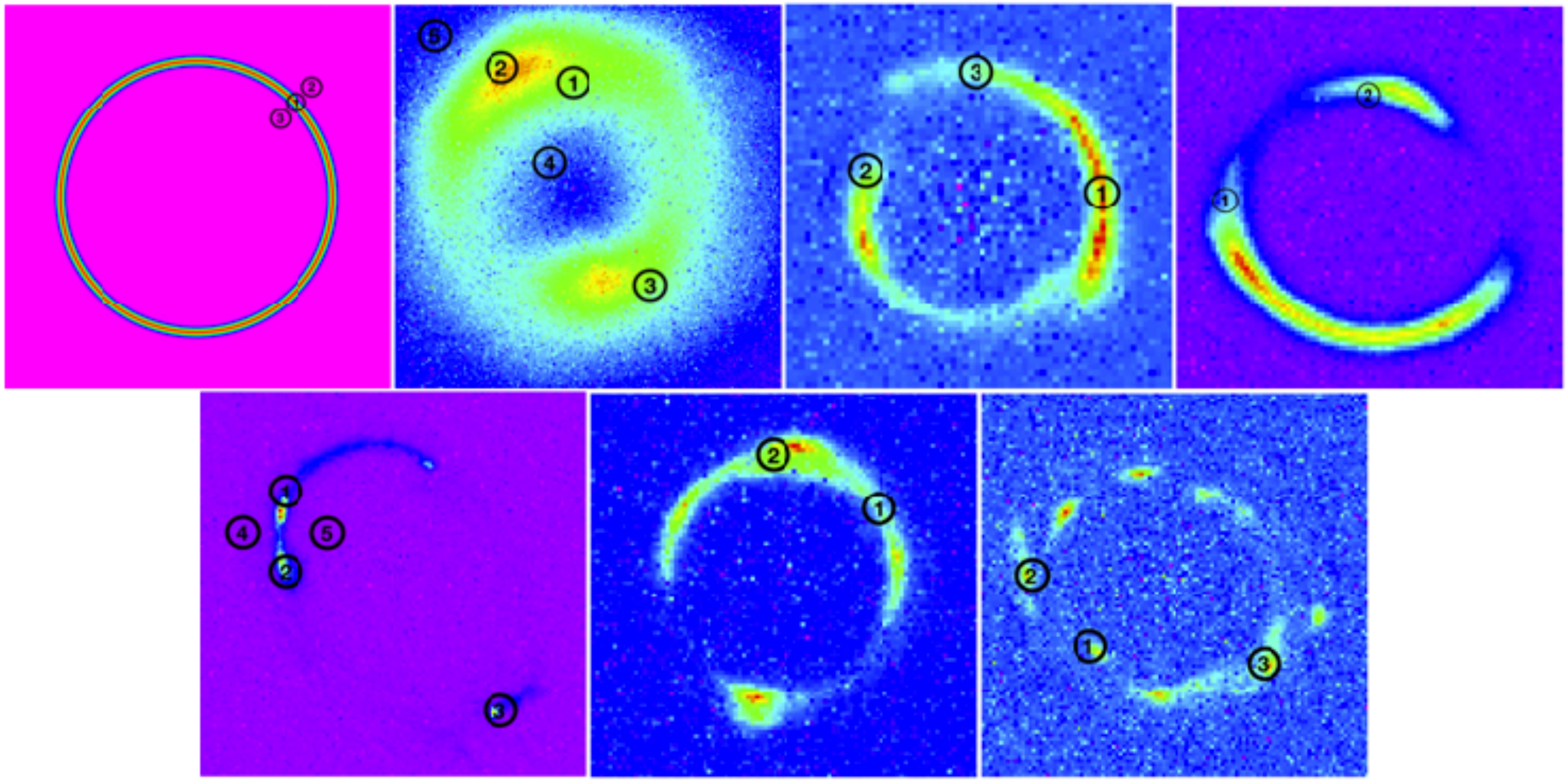

LOS contribution

$$\mathbf{u} = \mathbf{x} - \alpha_1(\mathbf{x}) - \alpha_2\left[\mathbf{x} - \beta\alpha_1(\mathbf{x})\right],$$

$$\mathrm{d}\alpha = \left(\frac{1}{N_{\mathrm{pix}}}\sum_{i=1}^{N_{\mathrm{pix}}}(\Delta\alpha_{\mathrm{LOS}} - \Delta\alpha_{\mathrm{sub}})^2\right)^{1/2},$$

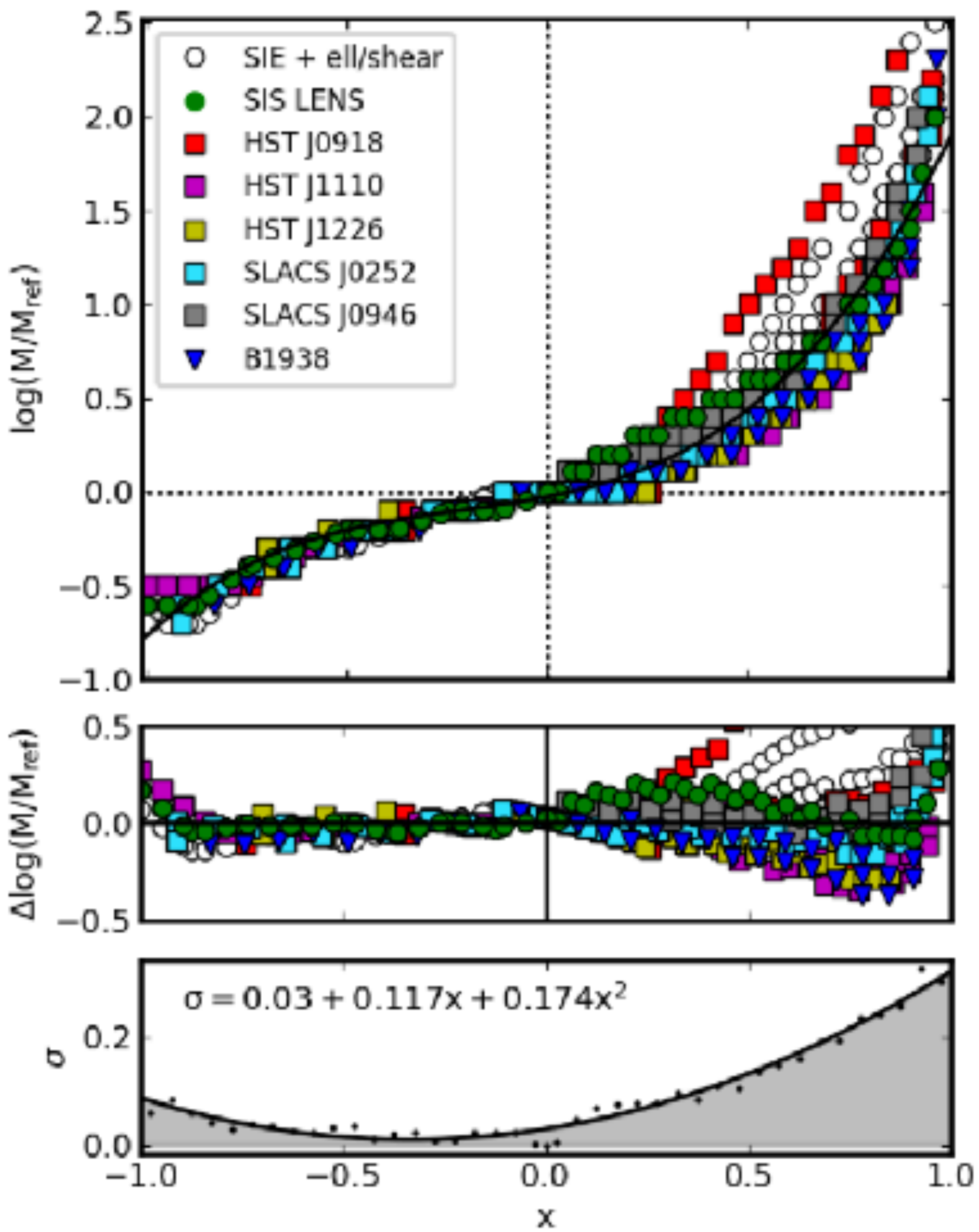

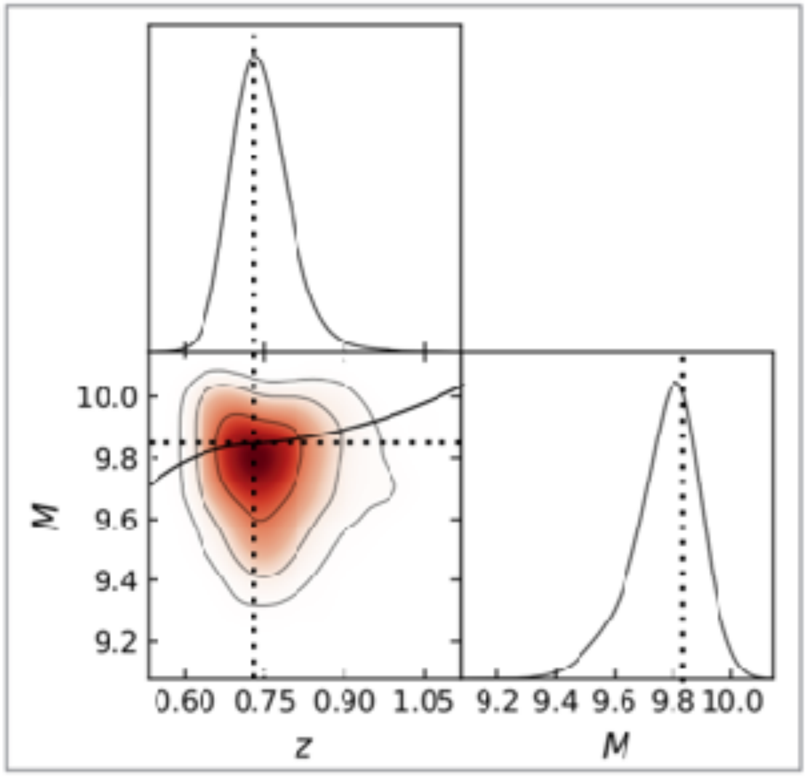

Despali, Vegetti et al. 2018

LOS contribution

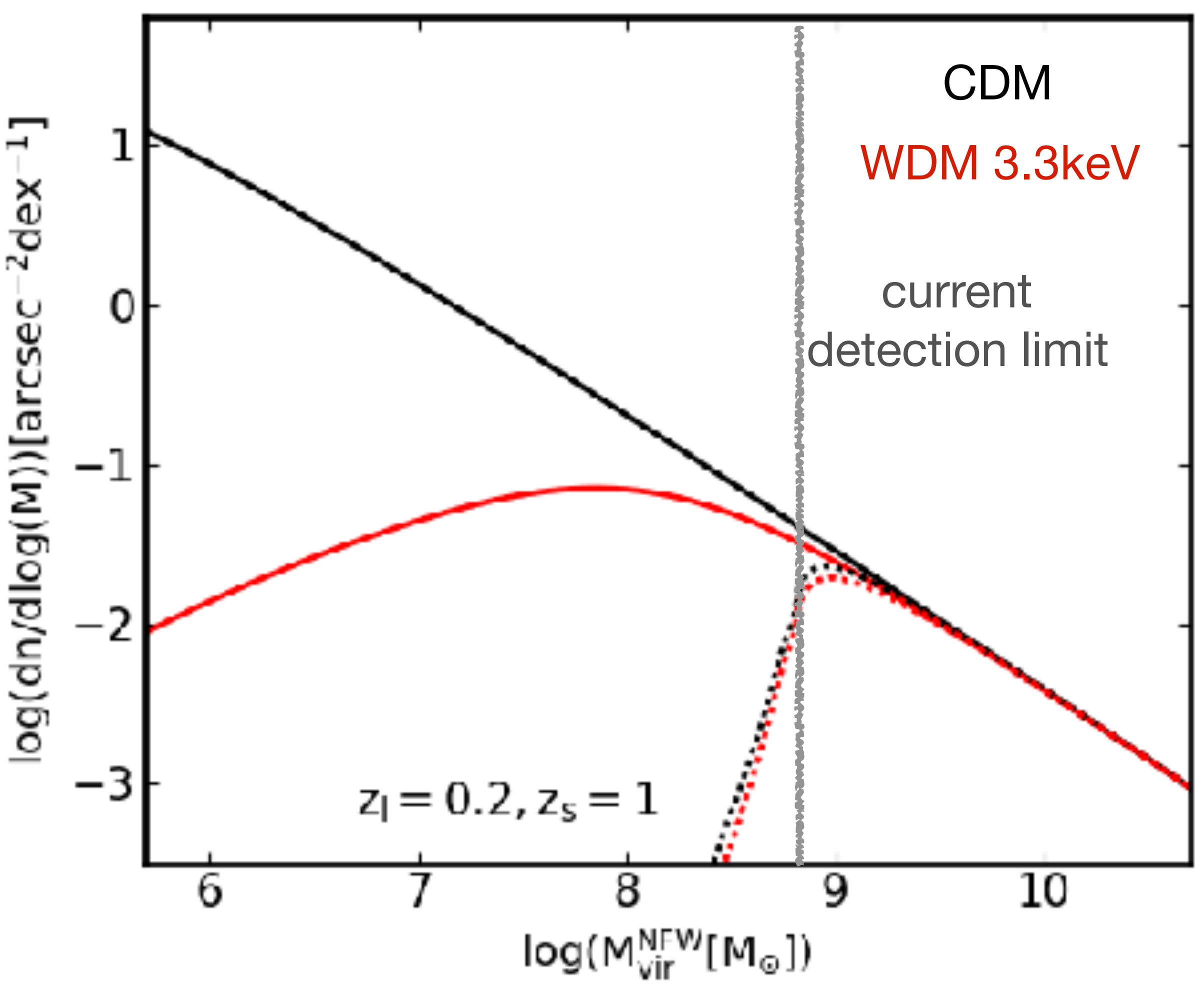

$$N_{LOS} = \int_0^{z_S} \int_{M_{LOW}(z)}^{M_{max}} n(m,z)\,dm \frac{dV}{dz}\,dz$$

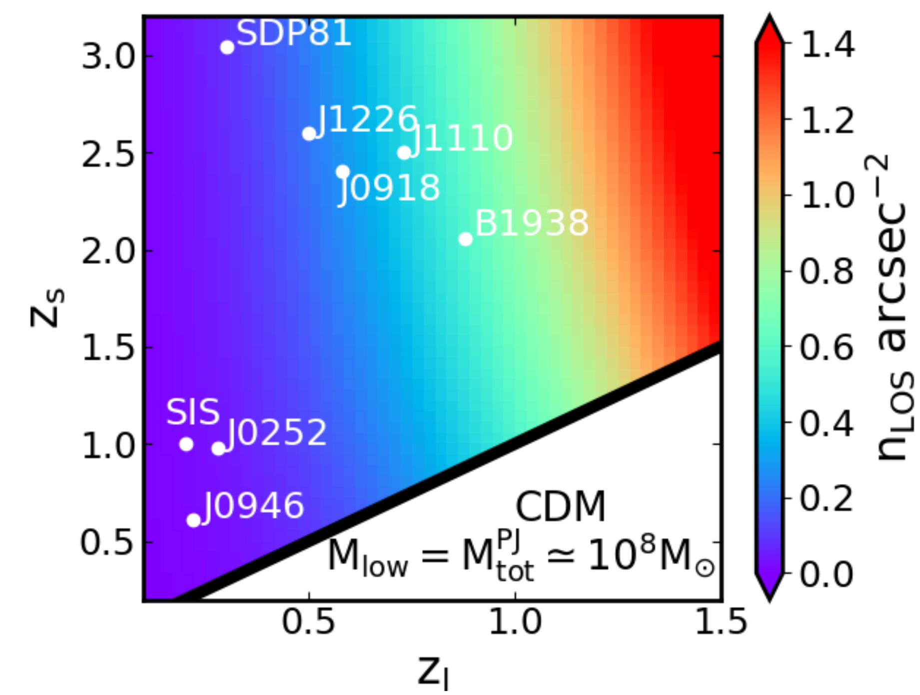

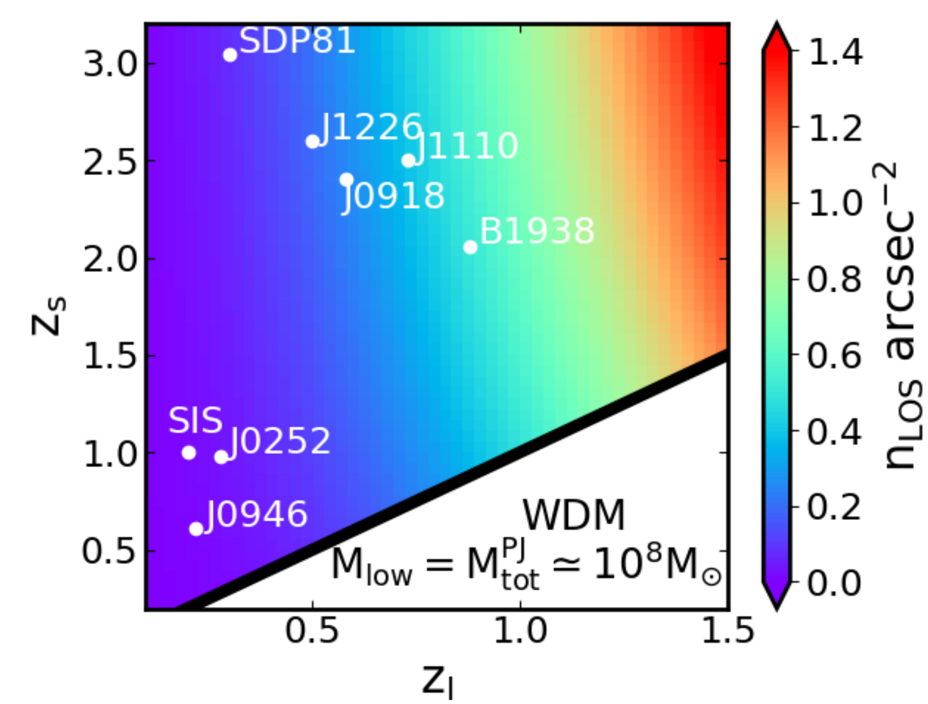

LOS contribution

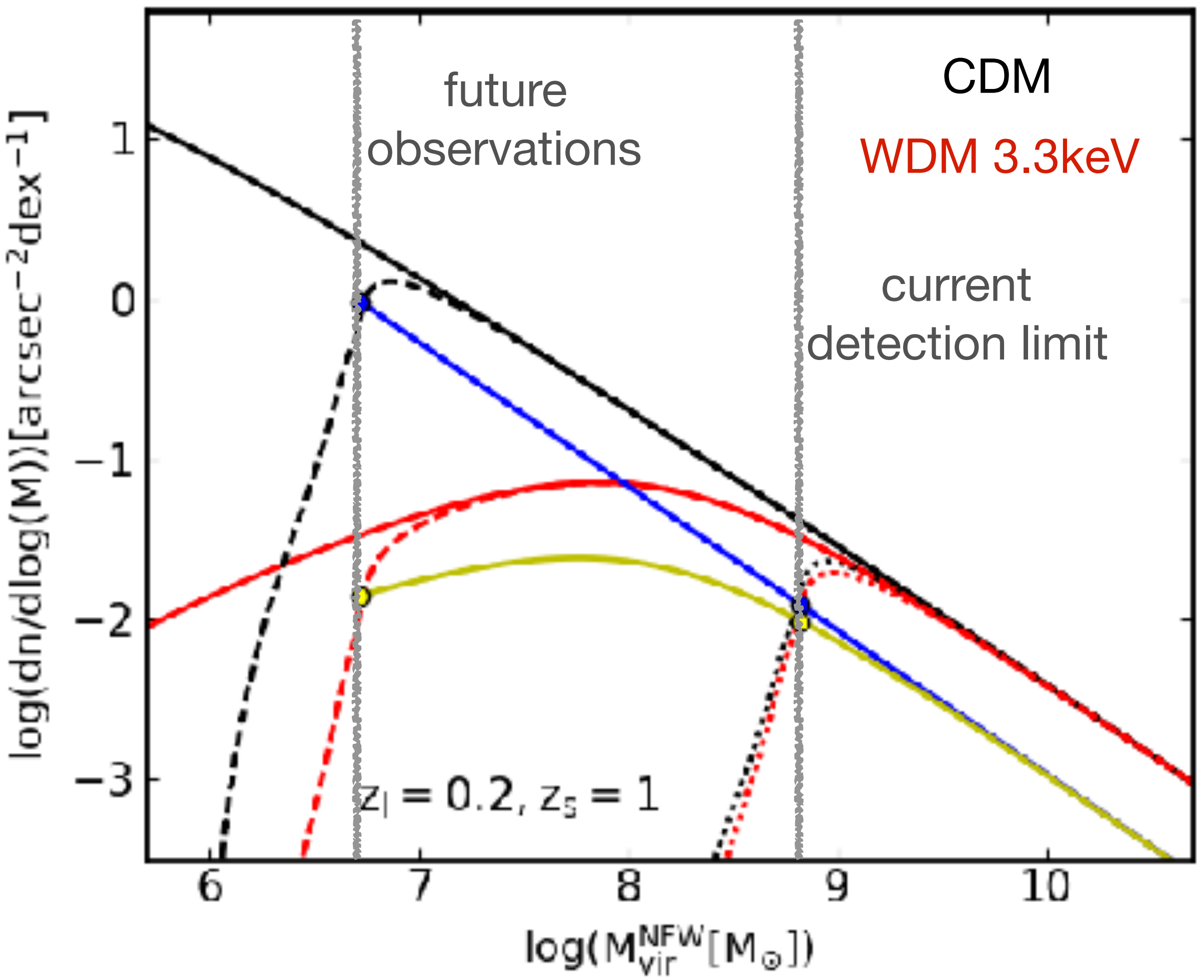

$$N_{LOS} = \int_0^{z_S} \int_{M_{LOW}(z)}^{M_{max}} n(m, z)\, dm \frac{dV}{dz} dz$$

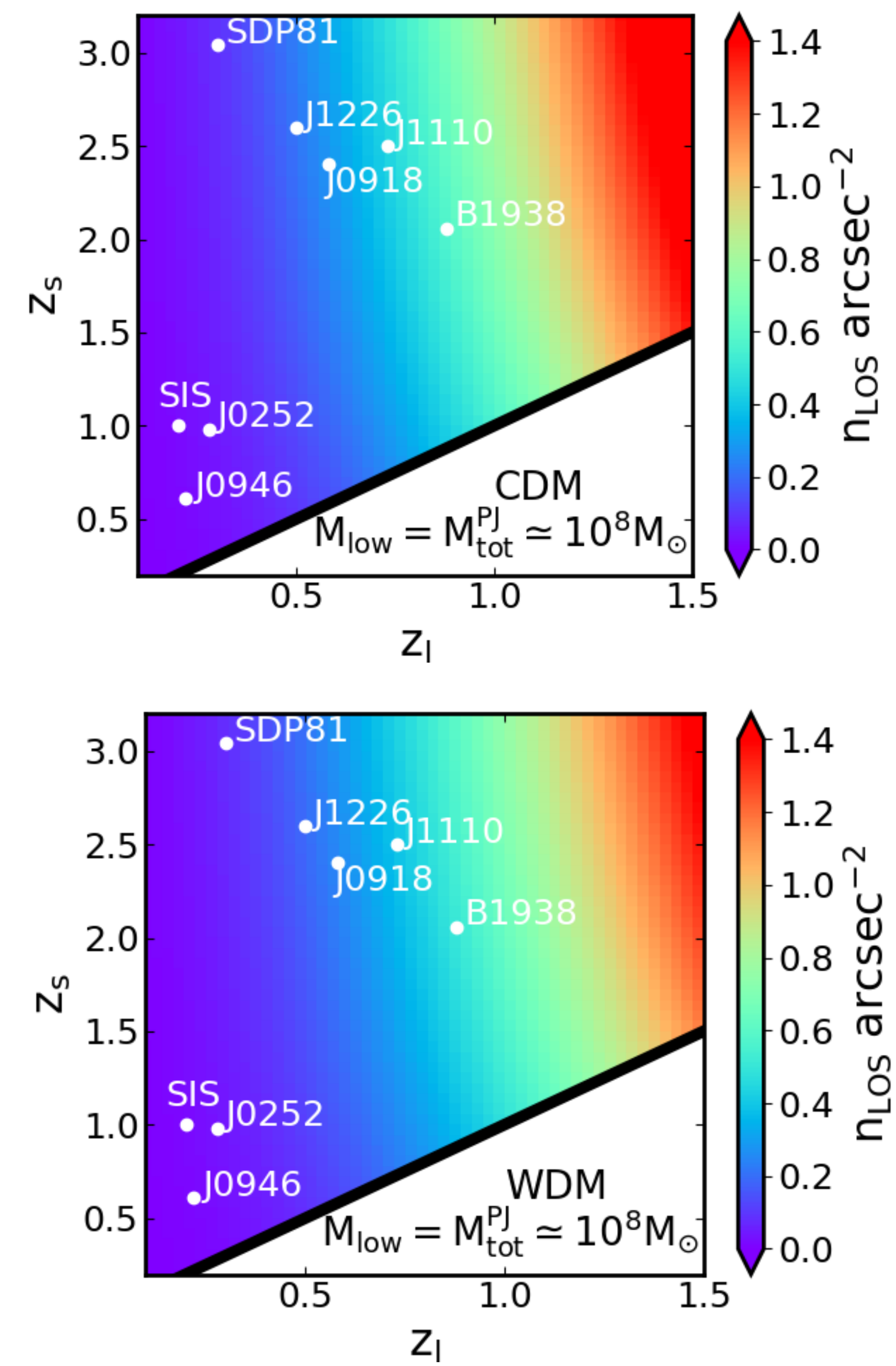

Observational Constraints I: Optical

Bolton+ 2006 Fassnacht+ 2017 Shu+ 2016

SLACS, SHARP & BELLS

SLACS

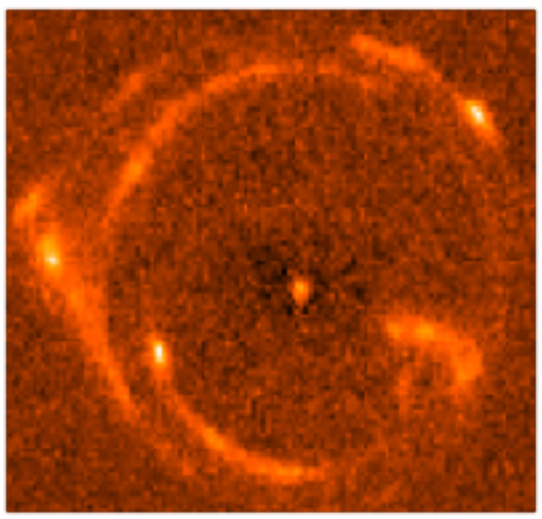

SDSS+HST

homogeneous sample of ~100 lenses

Lenses: z = 0.06 - 0.3 ET

Sources: z = 0.2 -1.0 SF

S. Sensitivity: $10^8 - 10^9 M_\odot$

SHARP

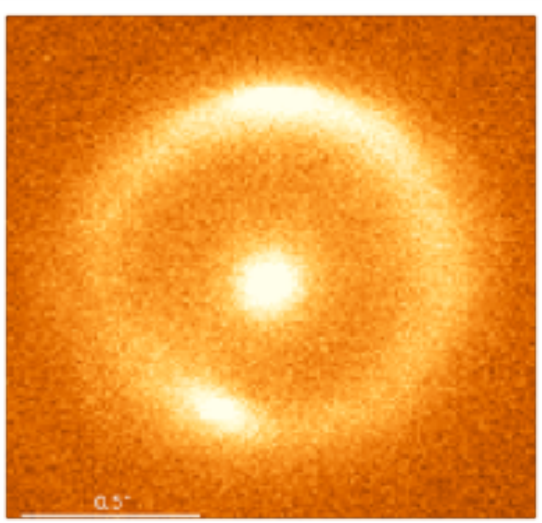

Keck II AO

inhomogeneous sample of ~30 lenses

Lenses: z = 0.1 - 0.6

Sources: z = 0.2 - 1.0

S. Sensitivity: $\sim 10^8 \odot$

BELLS

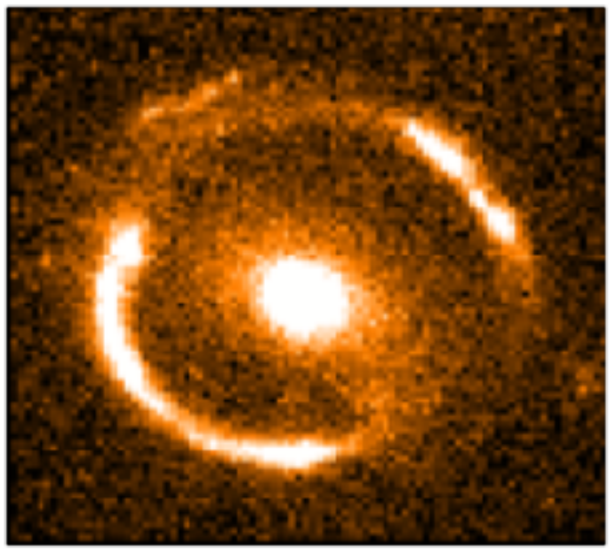

SDSS+HST

homogeneous sample of ~20 lenses

Lenses: z = 0.3 - 0.7 ET

Sources: z = 2.0 - 3.0 LAEs

S. Sensitivity: $10^8 - 10^9 M_\odot$

Vegetti + 2010

SLACS: First Detection

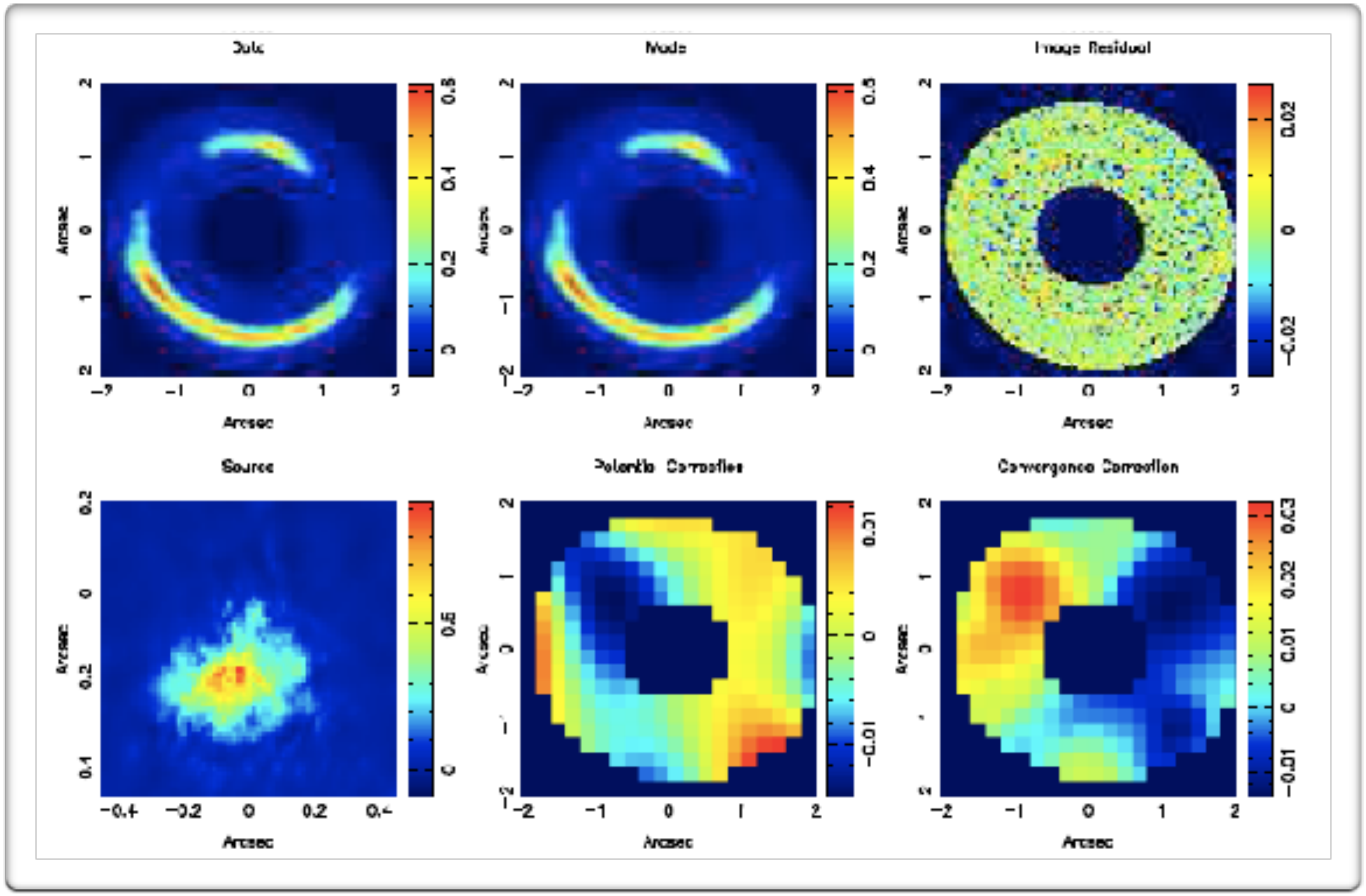

$$M_{\rm sub} = (3.51 \pm 0.15) \times 10^9 M_\odot$$

$$({\rm M/L})_{\rm V,\odot} \geq 120\ M_\odot/{\rm L}_{\rm V,\odot}$$

$$\Delta \log \mathcal{E} = -128.0$$

16 sigma detection

Vegetti + 2014

SLACS: Subsample

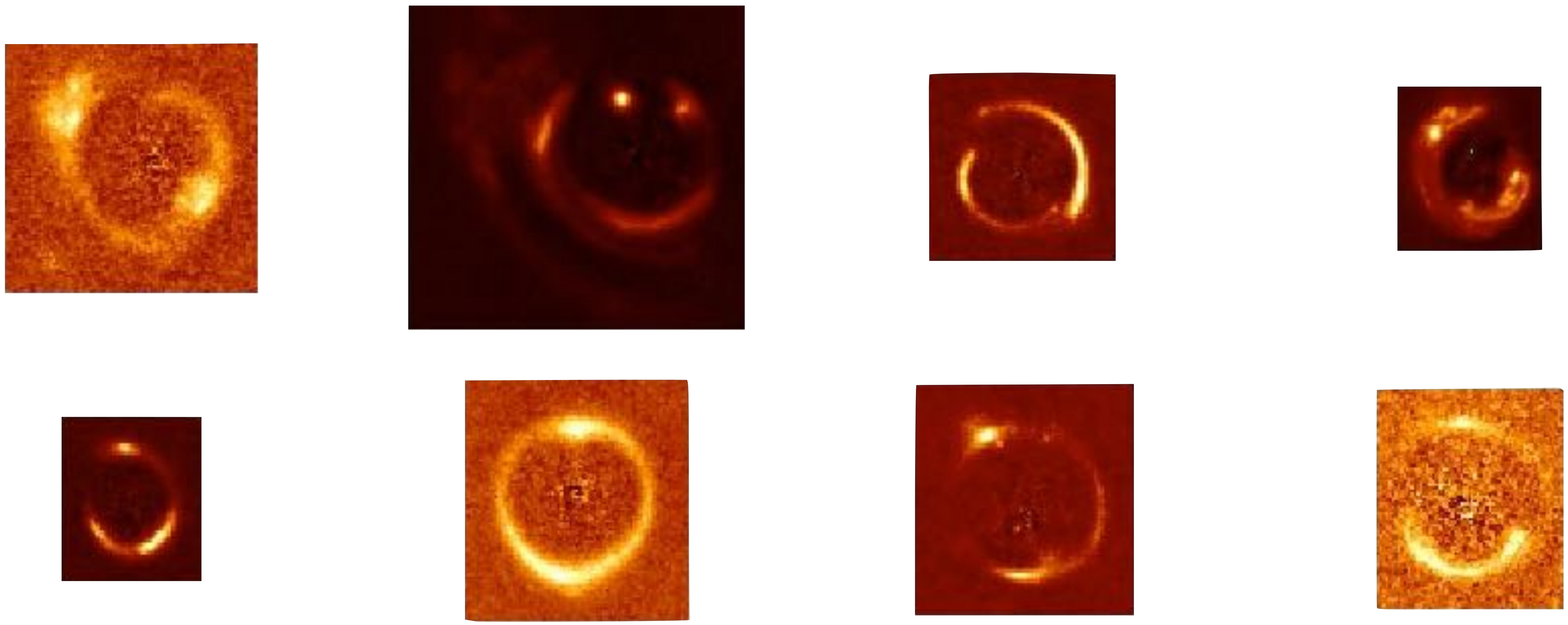

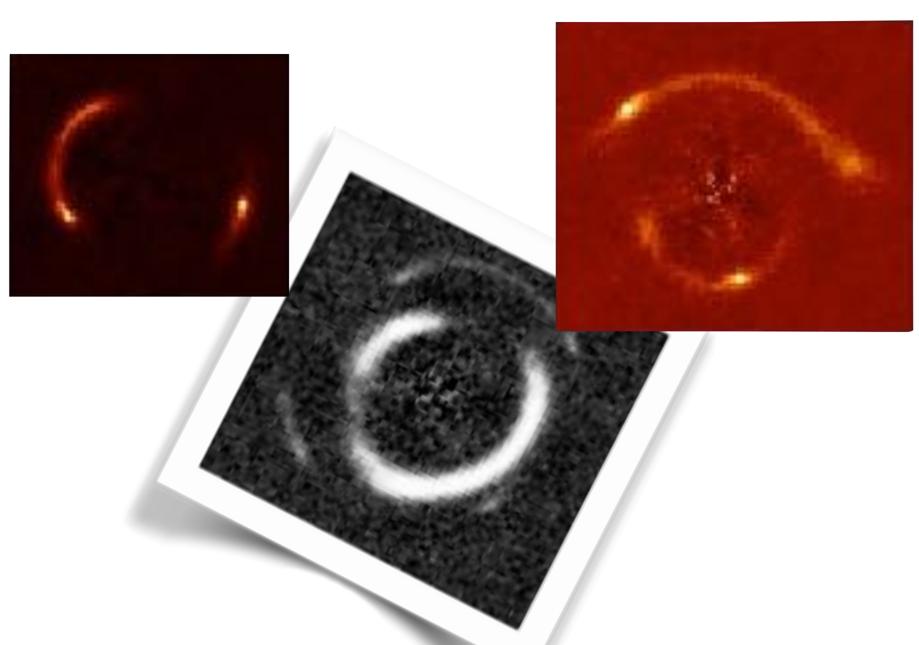

- Chosen on a s/n basis
- Representative sub-sample of the SLACS lenses
- Representative sample of massive early-type galaxies

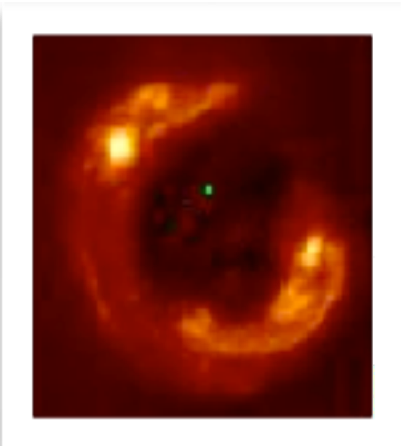

Sensitivity function

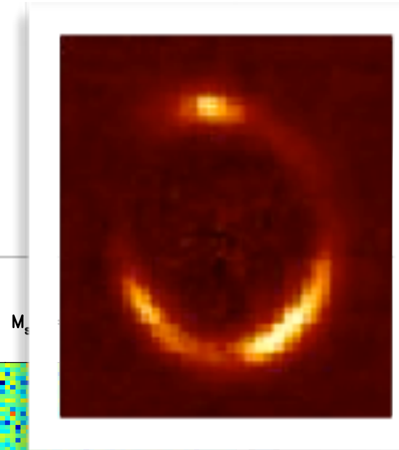

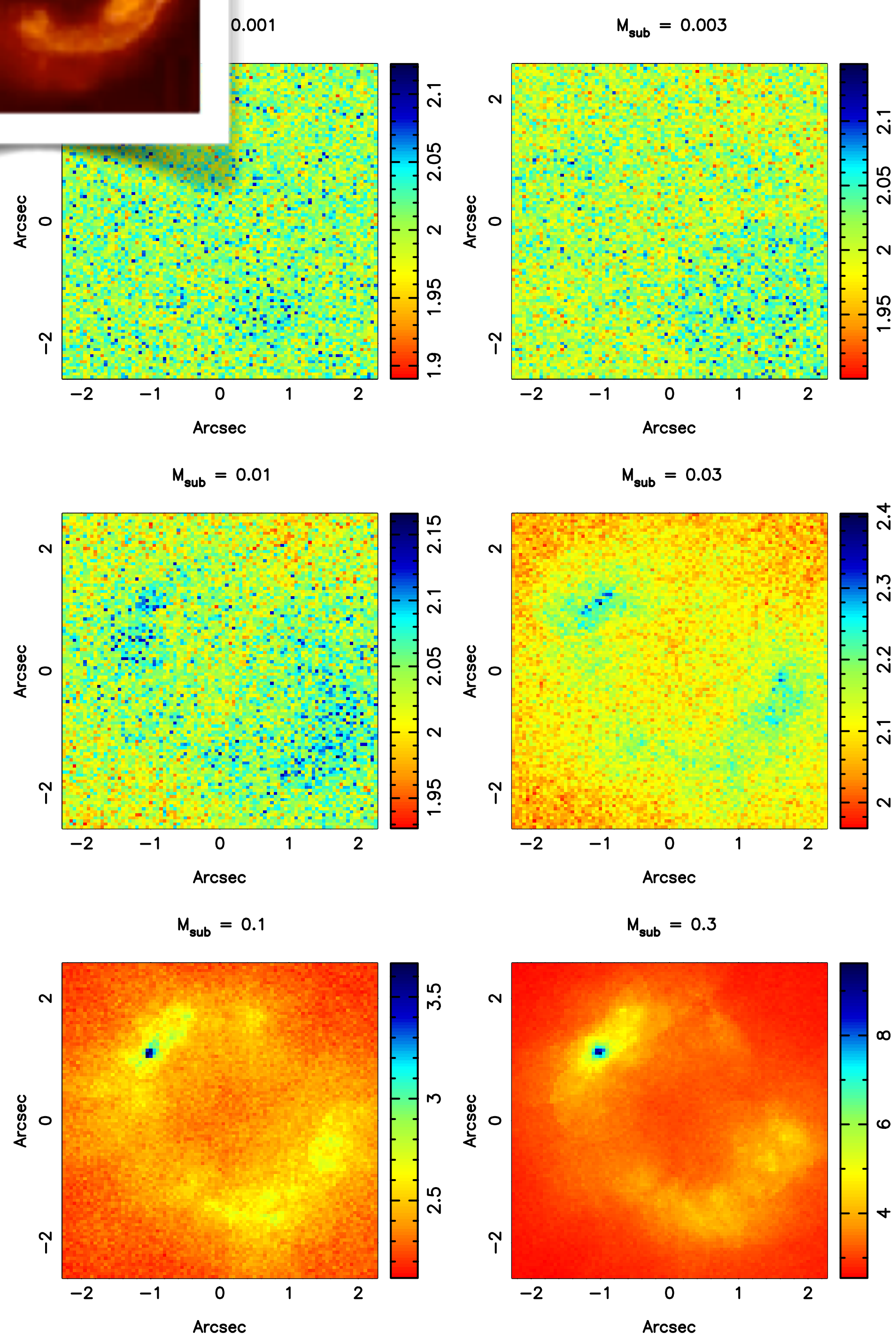

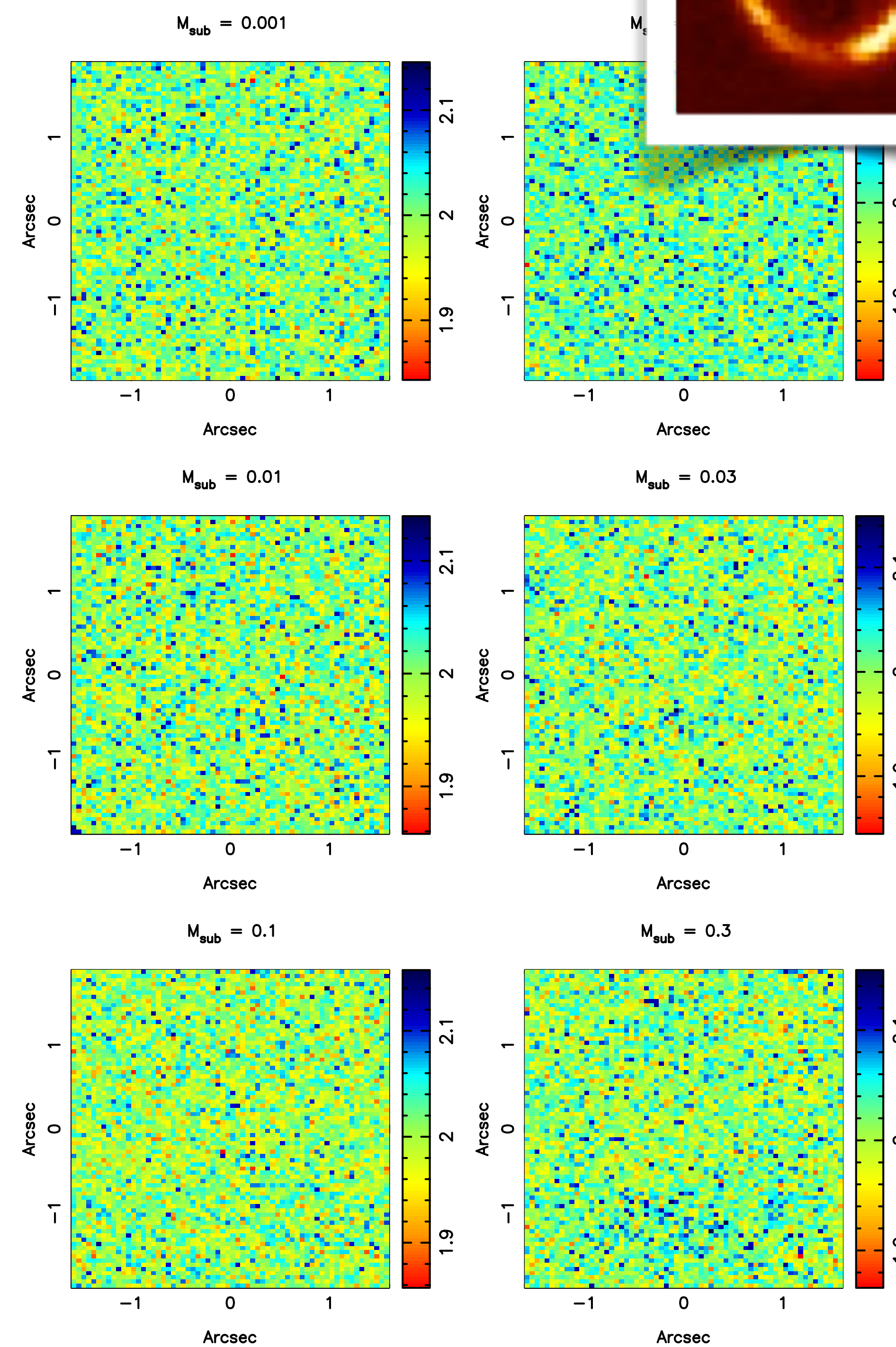

Vegetti+ 2014 Xu+ 2014

SLACS: First measure of the mass function

$$P\left(\alpha, f \mid \{n_s, \mathbf{m}\}, \mathbf{p}\right)$$

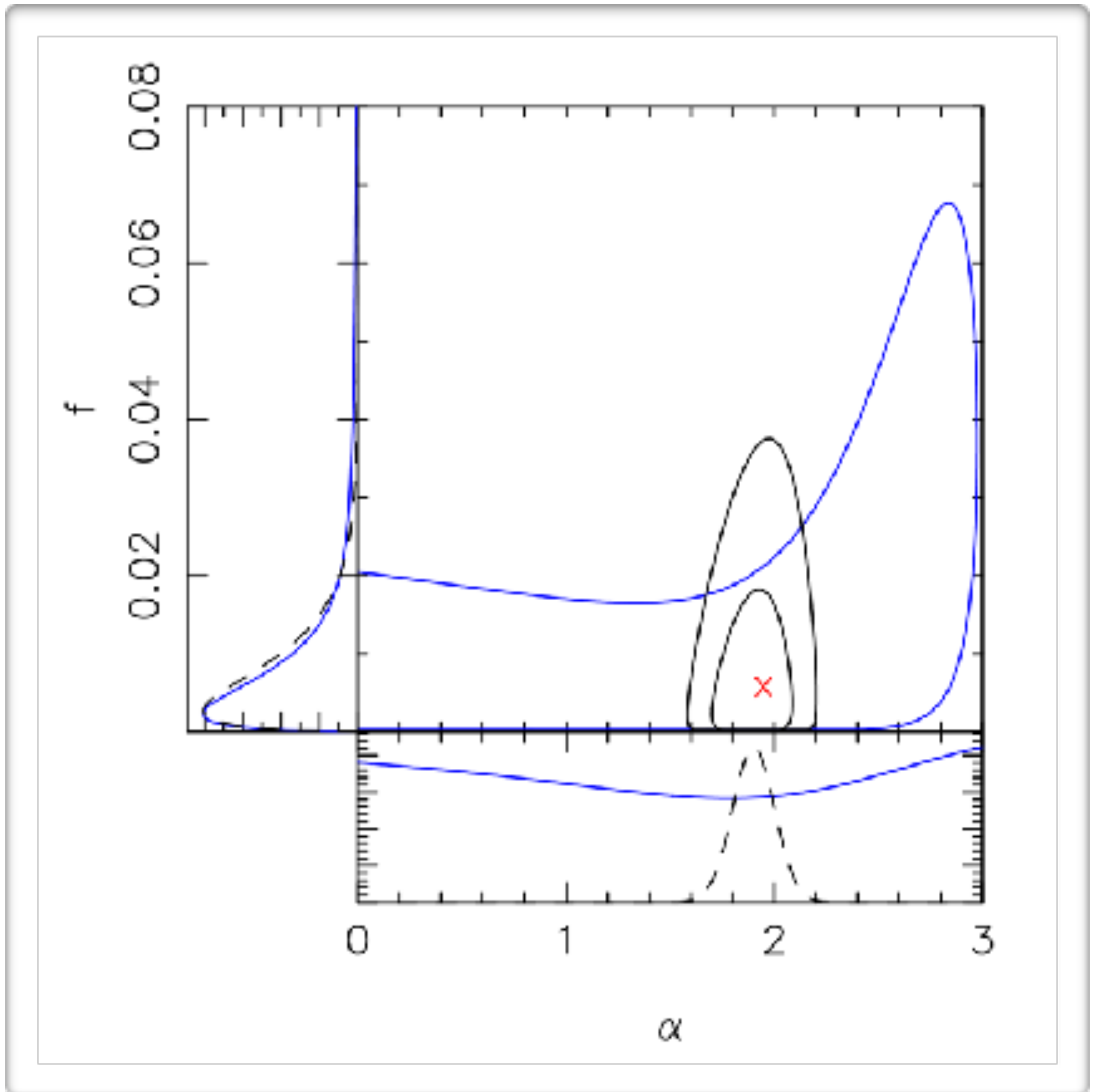

$$dN/dM \propto f M^{-\alpha}$$

Derived mass function parameters from a sample of 11 SLACS lenses

P(α)	f (68% CL)	α	ln Ev
U	$0.0076^{+0.0208}_{-0.0052}$	< 2.93 (95% CL)	-5.98
G	$0.0064^{+0.0080}_{-0.0042}$	$1.90^{+0.098}_{-0.098}$ (68% CL)	-6.13

Results are consistent with CDM predictions, but due to the low sensitivity they do not rule out Warm Dark Matter models

SLACS: constraints on sterile neutrinos

$$n(m) = n(m)^{\mathrm{CDM}} \left(1 + \frac{M_{\mathrm{hm}}}{m}\right)^{\beta}$$

$$\log P\left(\mathbf{m}^{\mathrm{o}}, \mathbf{X}^{\mathrm{o}} | \theta\right) = -\int \left[\mu_s(m^{\mathrm{o}}, \mathbf{x}^{\mathrm{o}}) + \mu_l(m^{\mathrm{o}}, \mathbf{x}^{\mathrm{o}})\right] dm^{\mathrm{o}} d\mathbf{x}^{\mathrm{o}} + \sum_i^n \log \left[\mu_s\left(m_i^{\mathrm{o}}, \mathbf{x}_i^{\mathrm{o}}\right) dm^{\mathrm{o}} d\mathbf{x}^{\mathrm{o}} + \mu_l\left(m_i^{\mathrm{o}}, \mathbf{x}_i^{\mathrm{o}}\right) dm^{\mathrm{o}} d\mathbf{x}^{\mathrm{o}}\right] .$$

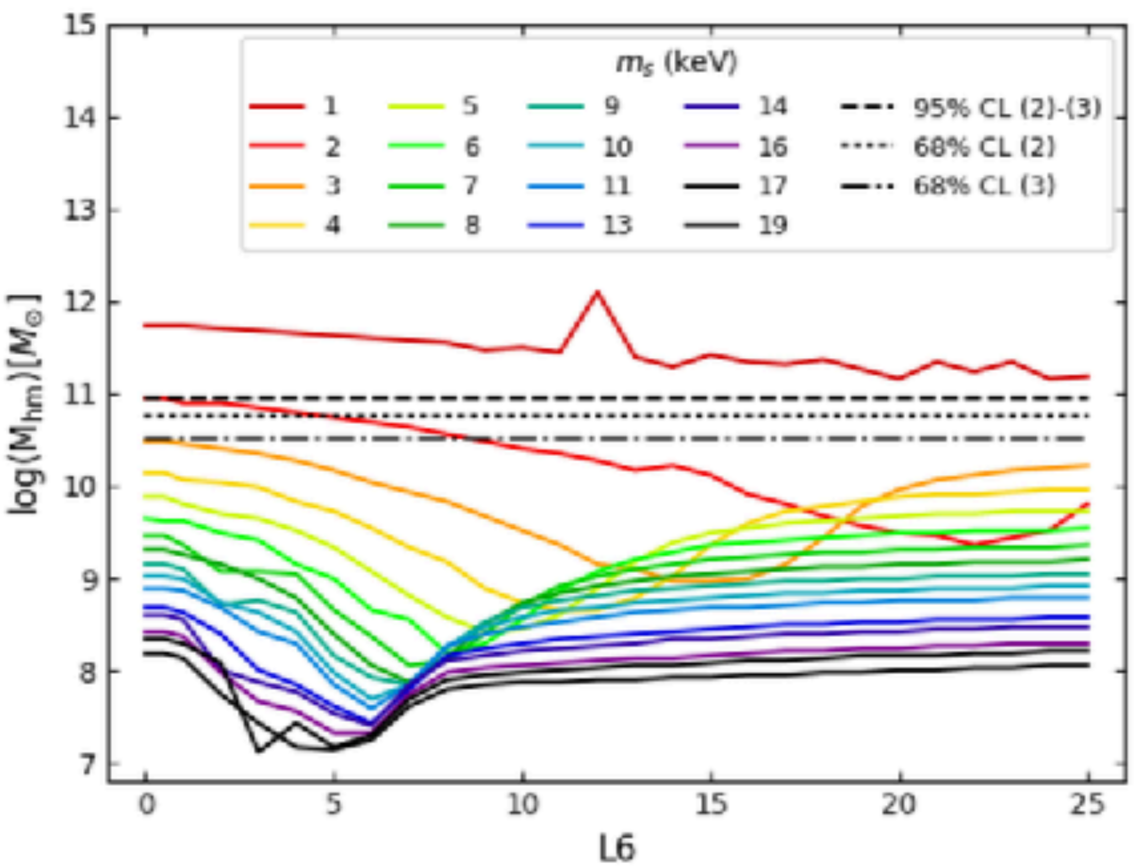

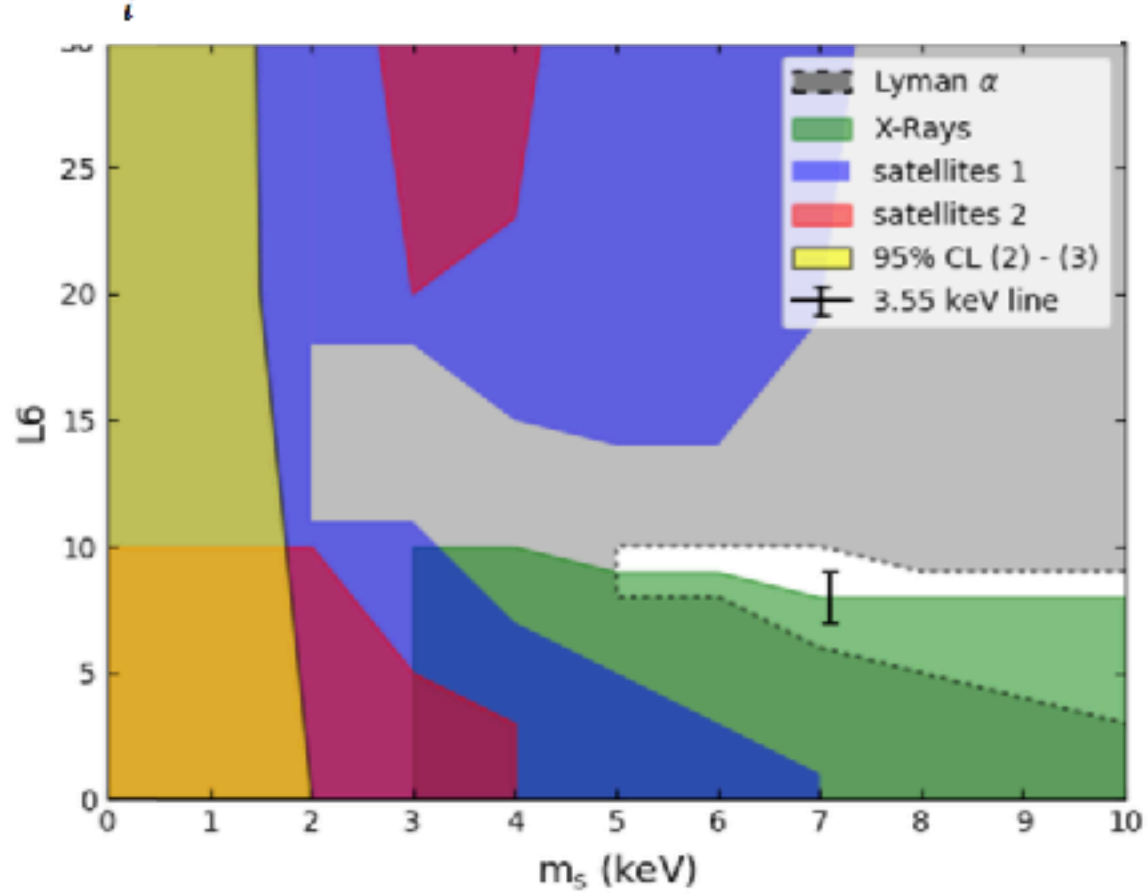

Expected CDM LOS: 1.6

BELLS

Increased data complexity leads to an increase in substructure sensitivity, higher redshift means higher LOS contribution

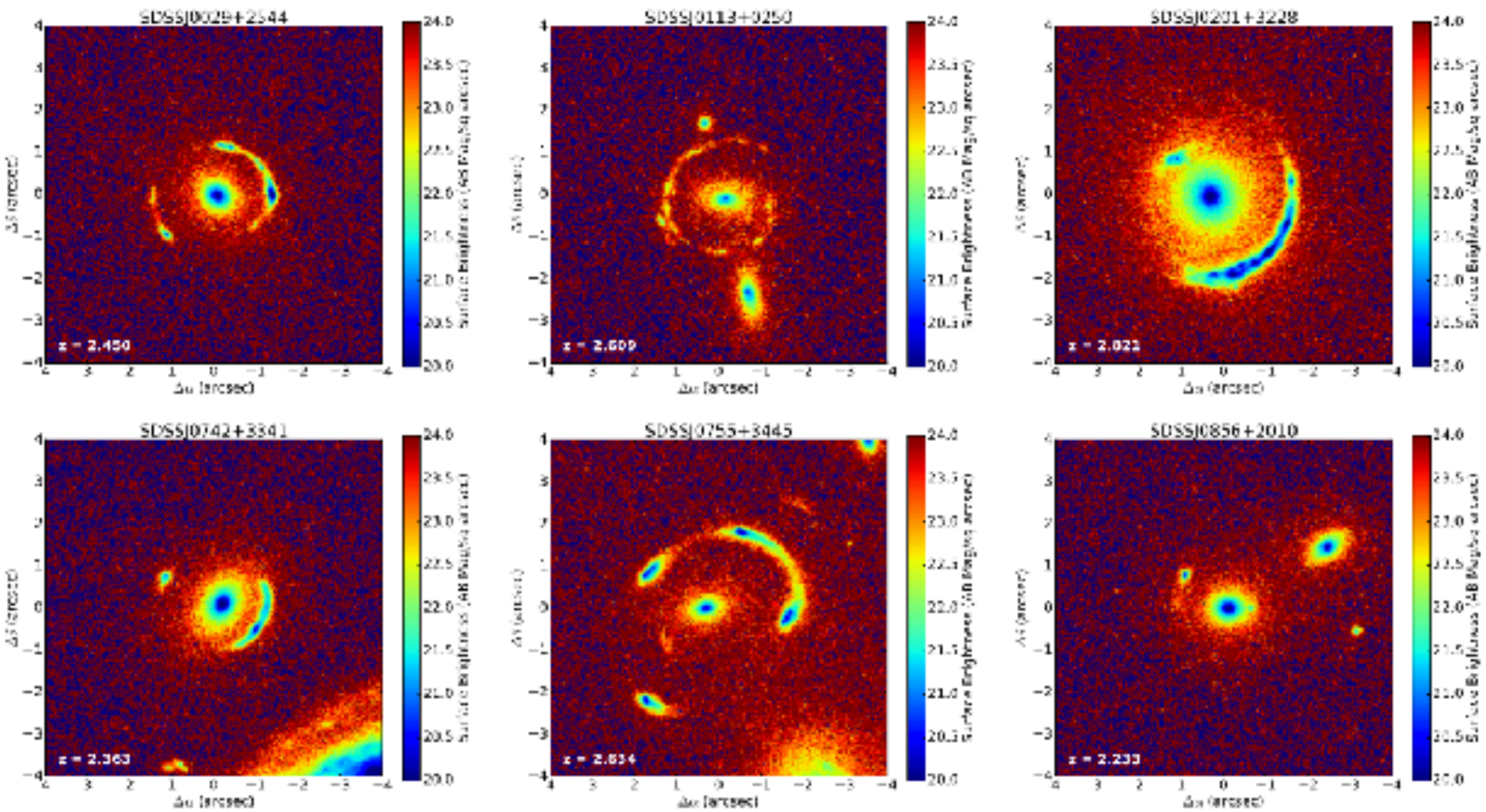

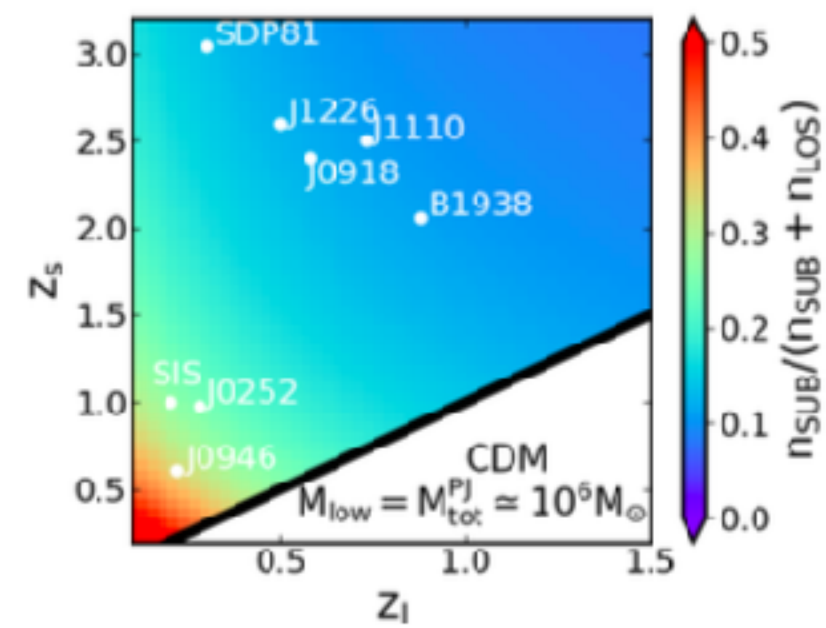

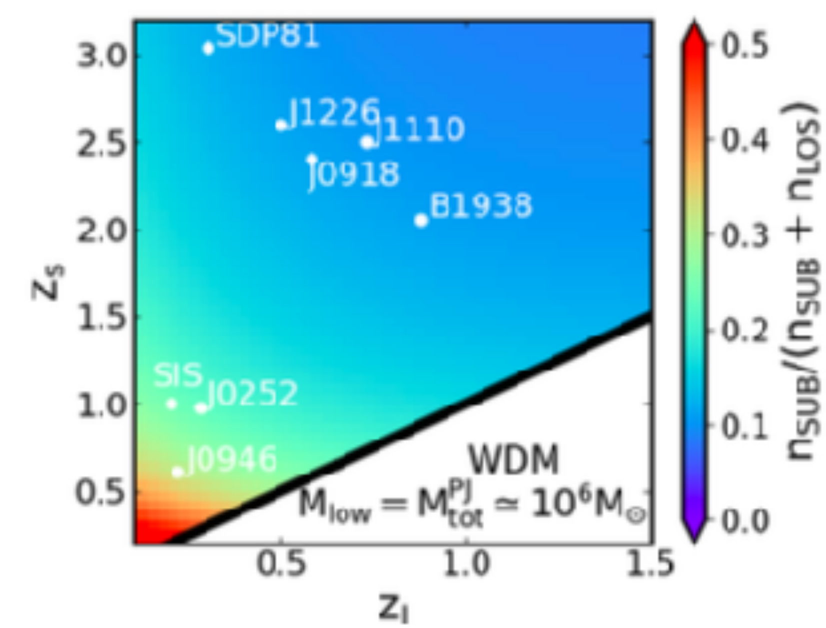

CDM

$$M_{\rm low} = 10^9 M_\odot \quad \mu_{\rm los} \sim 1.5$$

$$M_{\rm low} = 10^8 M_\odot \quad \mu_{\rm los} \sim 22$$

Lagattuta + 2012; Fassnacht + 2017 Vegetti + 2012; Hsueh+2016; Spingola + 2017; Vegetti + 2017; Ritondale+2017

SHARP

Increased angular resolution leads to an increase in substructure sensitivity

HST

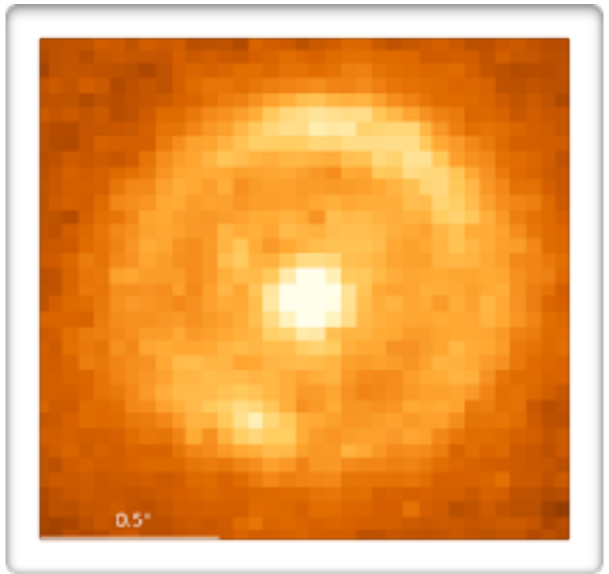

Keck Adaptive Optics

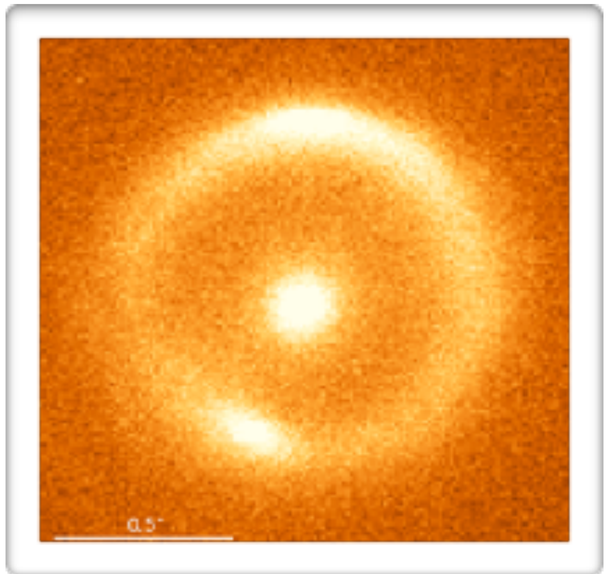

SHARP goals beyond substructure: probing the evolution of the FP, investigating the properties of of quasar host galaxies, quantifying systematics in flux ratio anomalies studies of gravitationally lensed quasars;

Vegetti + 2012

SHARP first detection at z=0.9

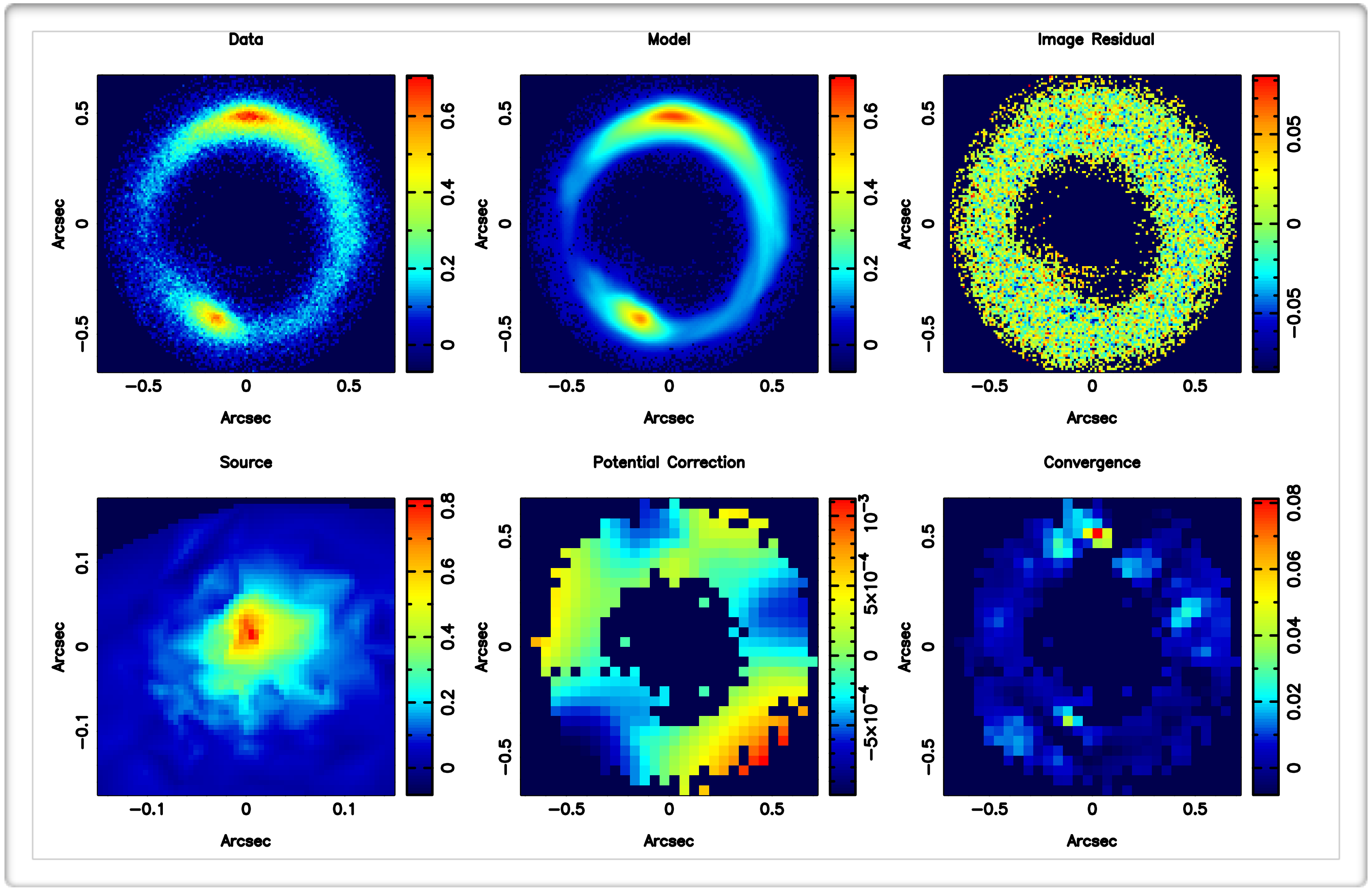

Vegetti + 2012

SHARP first detection/z=0.9

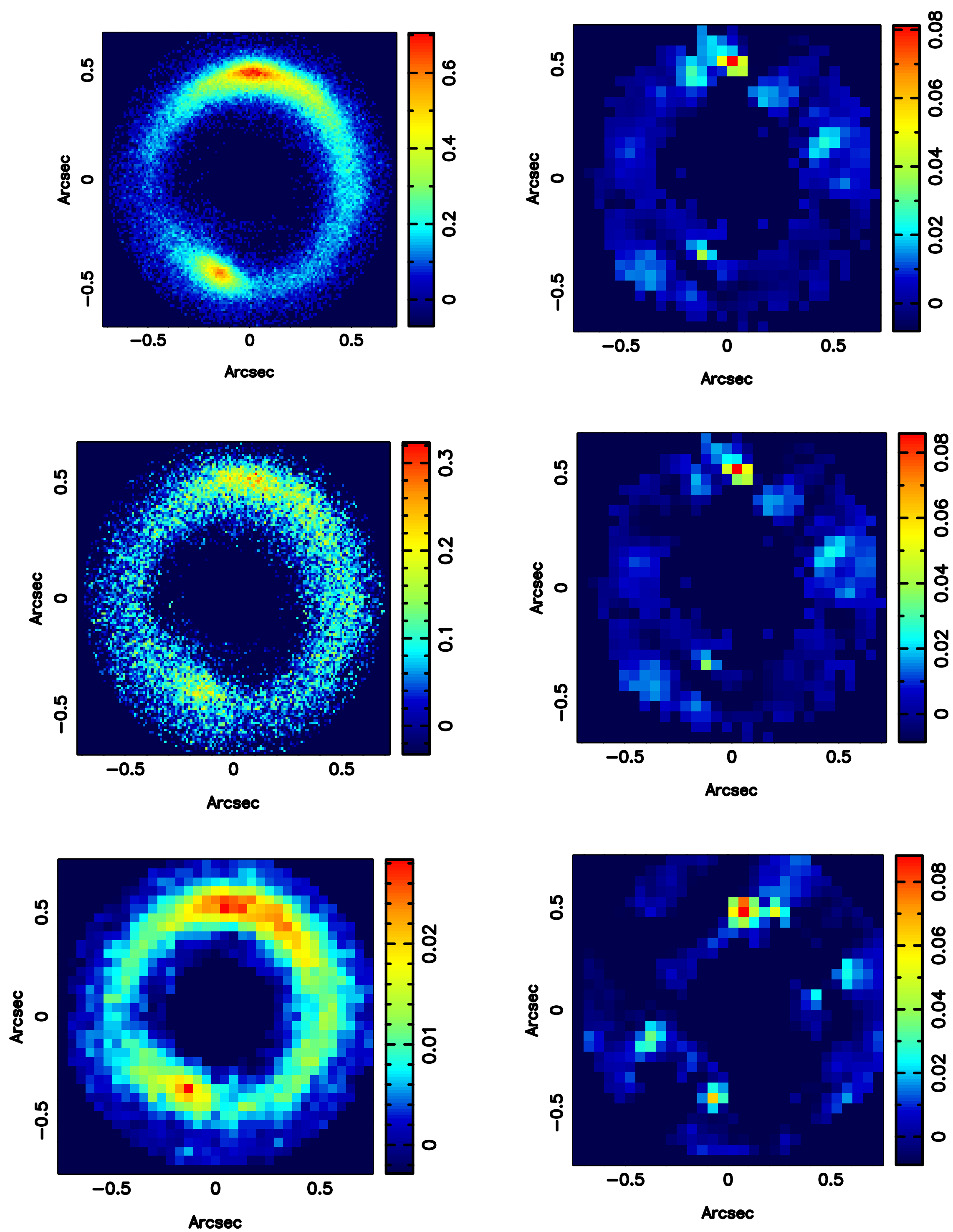

12 sigma detection per data set

$$M_{sub} = (1.9 \pm 0.1) \times 10^8 M_\odot$$

$$M(< 0.6) = (1.15 \pm 0.06) \times 10^8 M_\odot$$

$$M(< 0.3) = (7.24 \pm 0.6) \times 10^7 M_\odot$$

The quest for the smallest structure

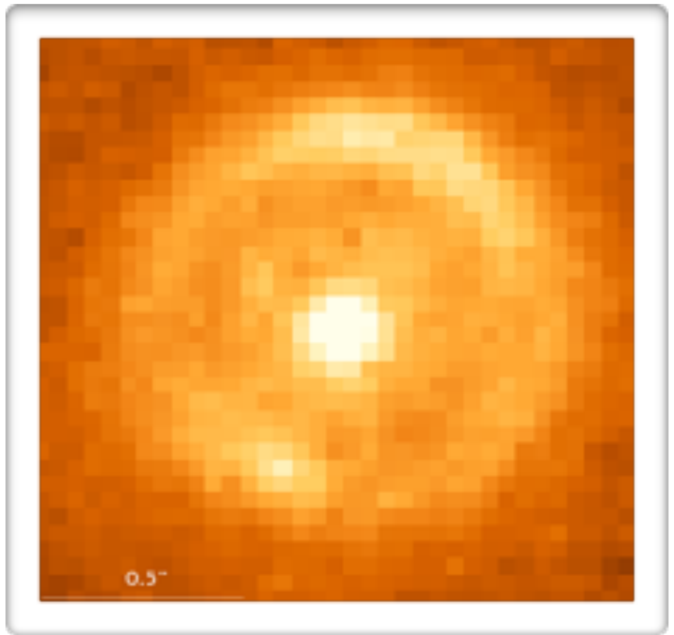

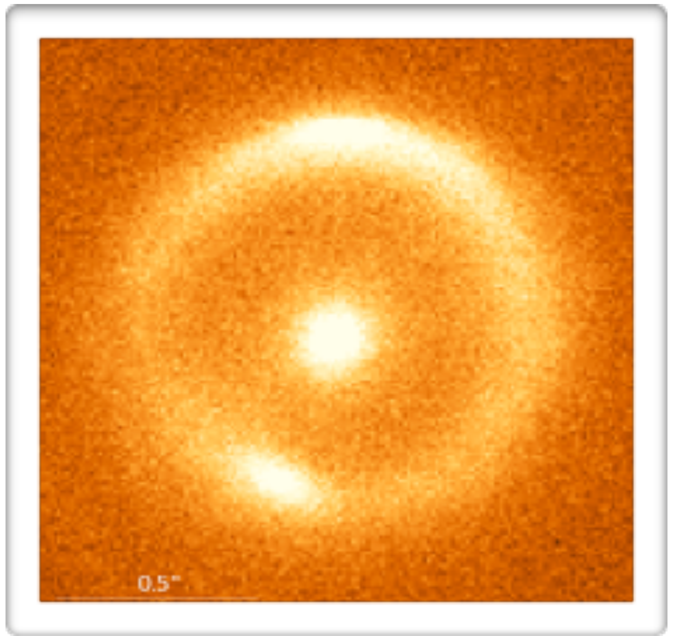

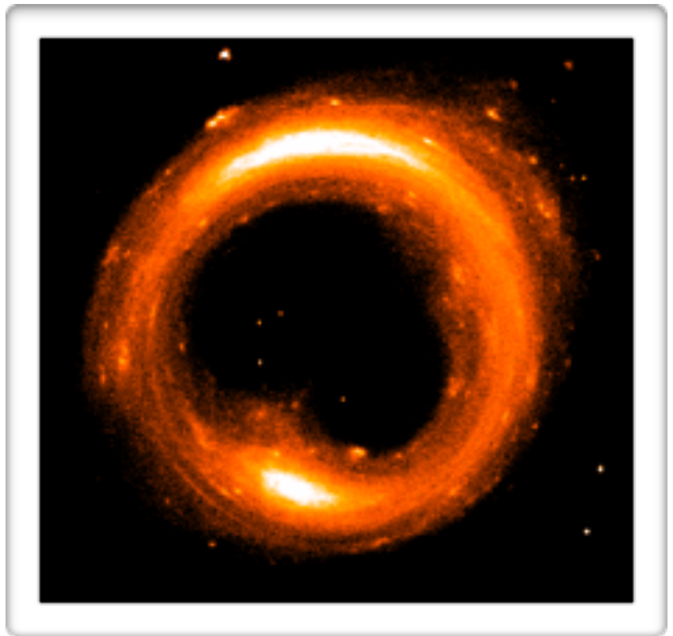

HST

10^9 M_{sun}

Keck AO

10^8 M_{sun}

E-ELT

?

Observational Constraints II: Interferometers

Interferometers

Global VLBI
Beam size ~1 mas
M(sub) ~ 10^6 M_{sol}

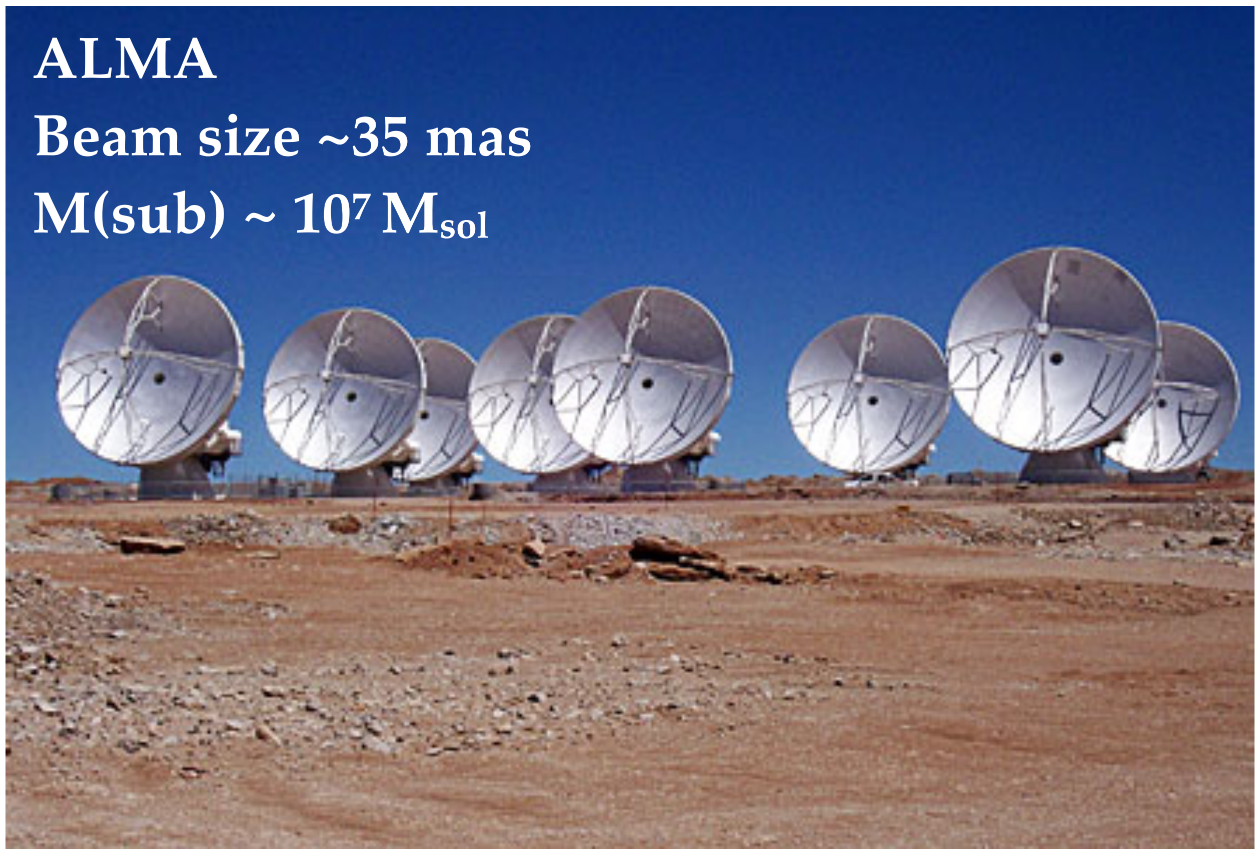

The quest for the smallest substructure

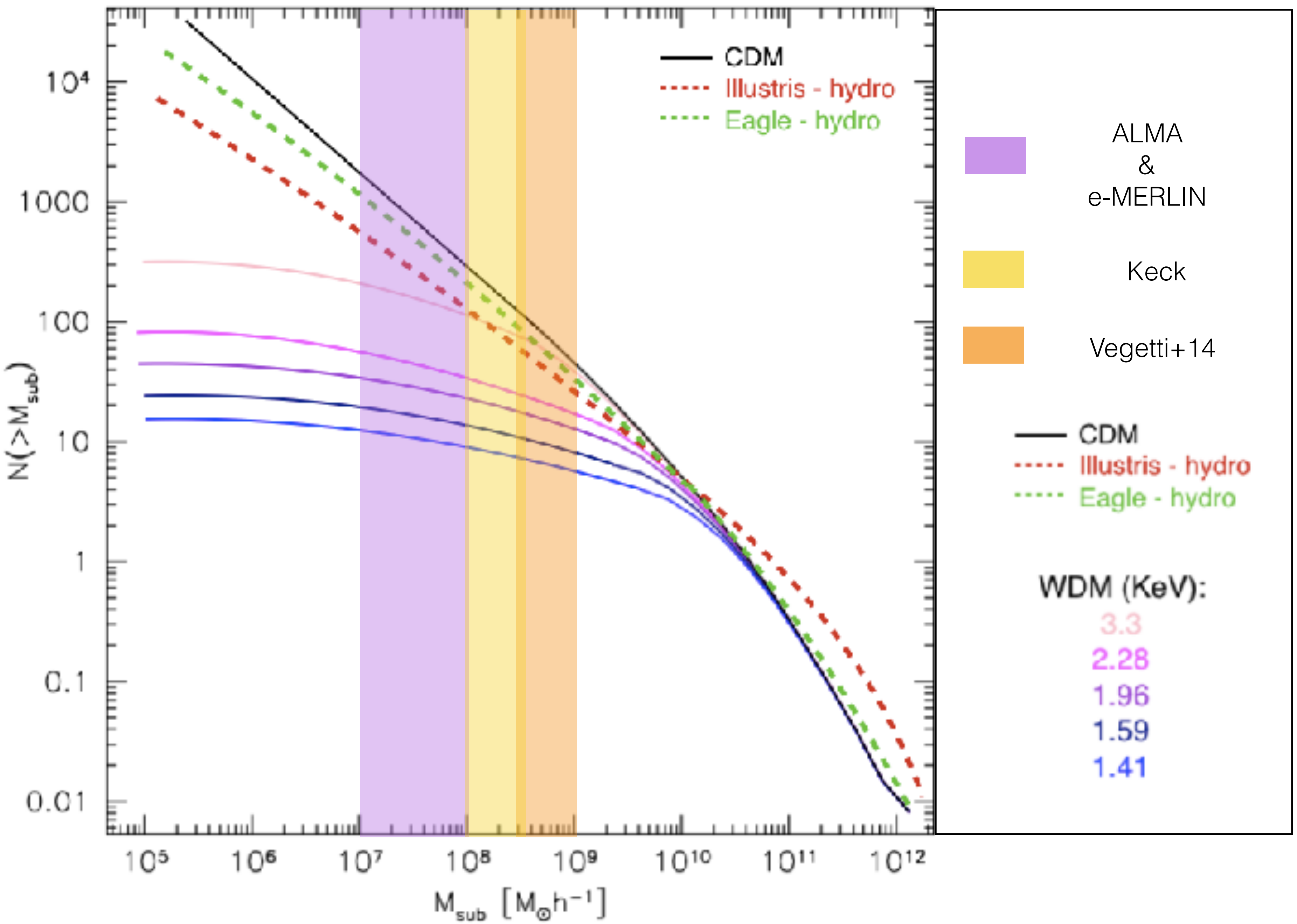

High-resolution data - low masses

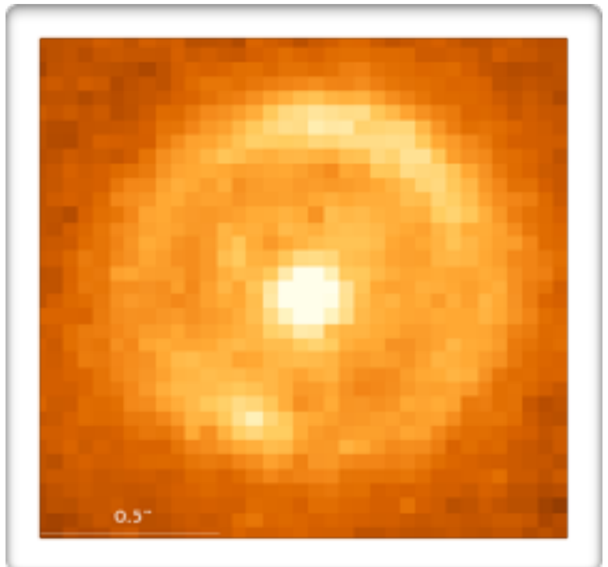

HST

10^9 M_{sun}

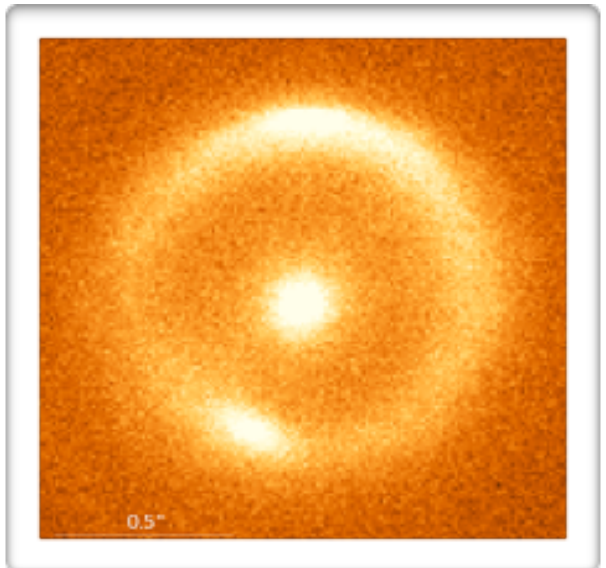

Keck AO

10^8 M_{sun}

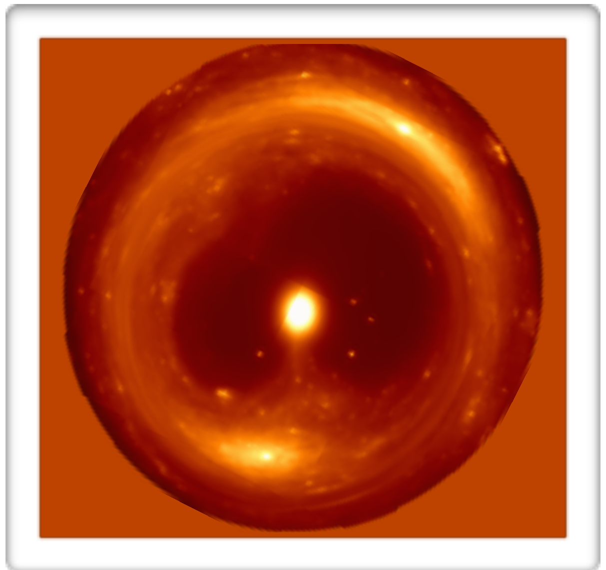

E-ELT

?

NOW

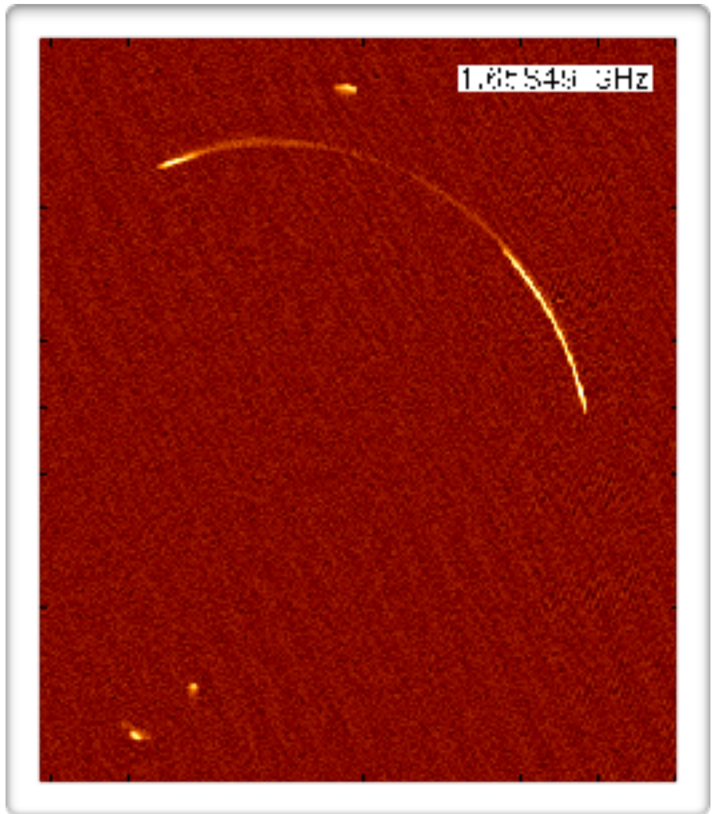

GVLBI

10^7-10^6 M_{sun}

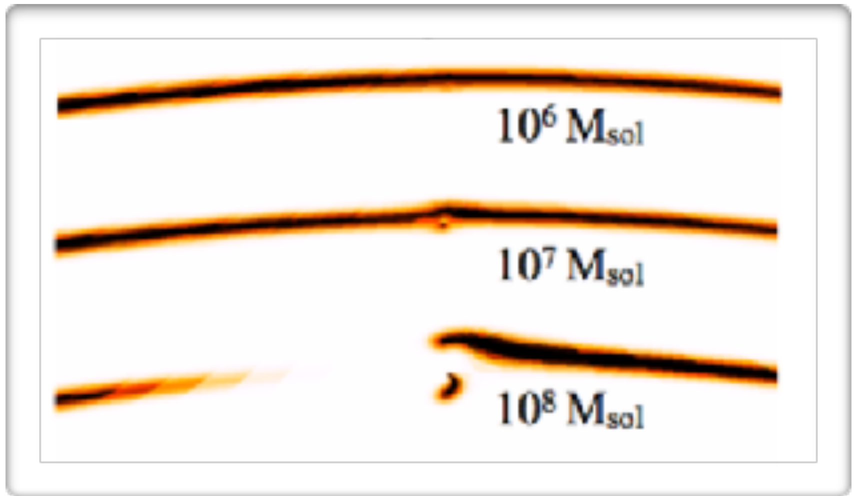

Gravitational Imaging in the UV plane

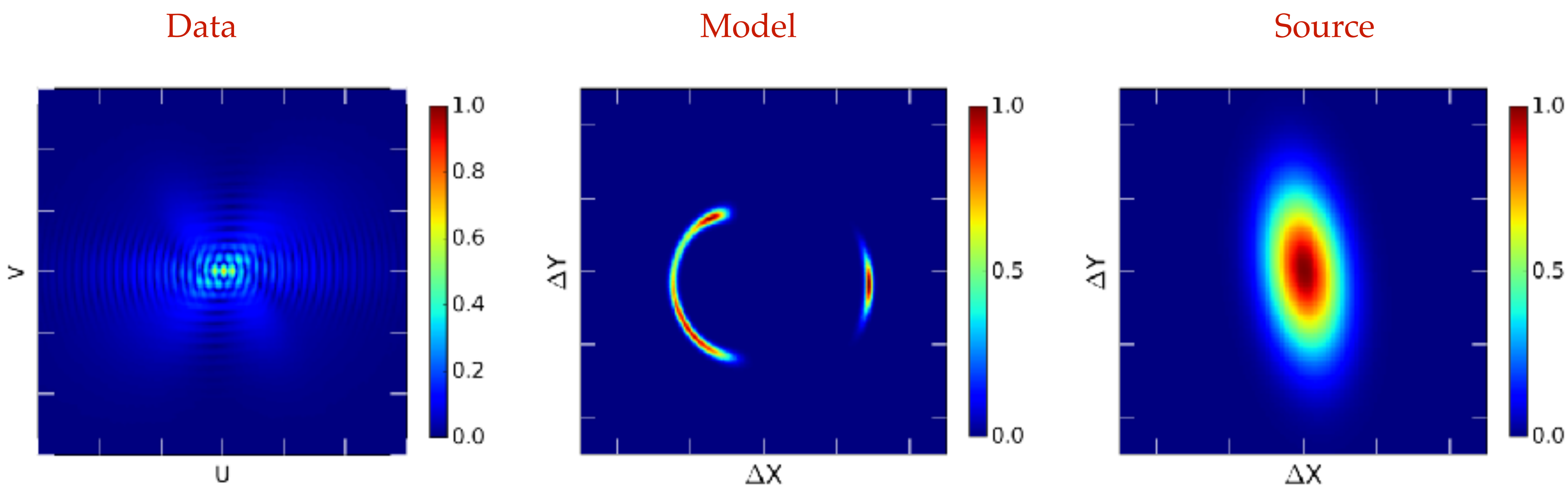

$$P = \chi^2 + \lambda_s^2\, \mathbf{H_s^T H_s s}$$

Needs to be defined in the visibility space

- Modelling of CLEANED images leads to unreliable source reconstructions
- Pixellated sources are key to study high-z lensed galaxies
- The quality of reconstructed sources strongly depends on the UV coverage

Projected results

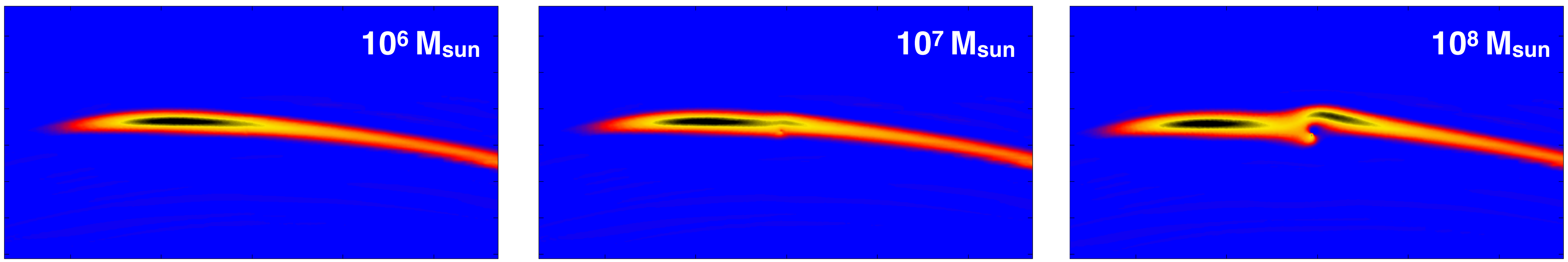

Expected constraints on the SBHMF from a sample of 4 VLBI lenses

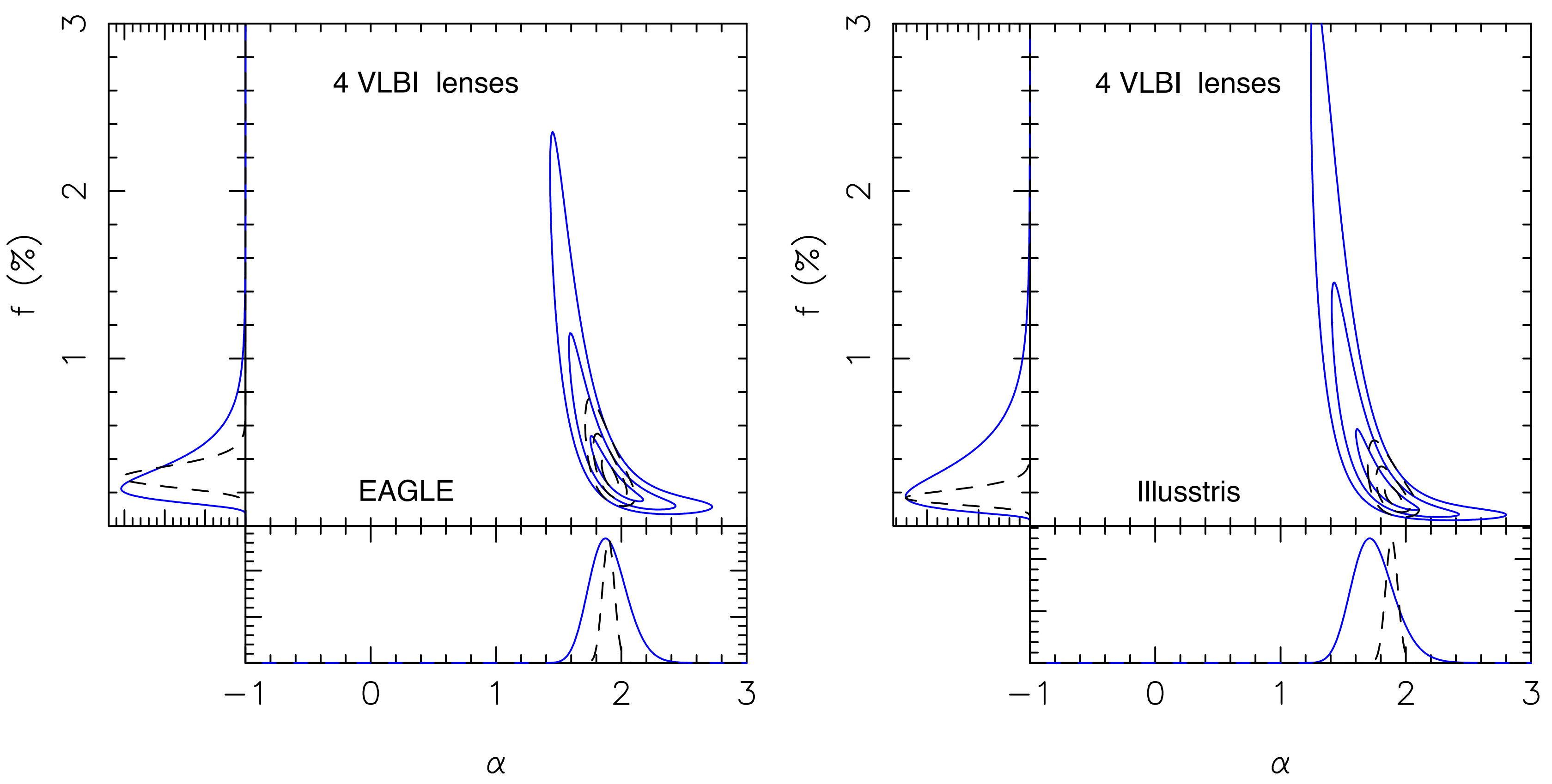

Multiple frequencies

Multiple frequencies can be used to i) increase sensitivity, ii) check for calibration errors.

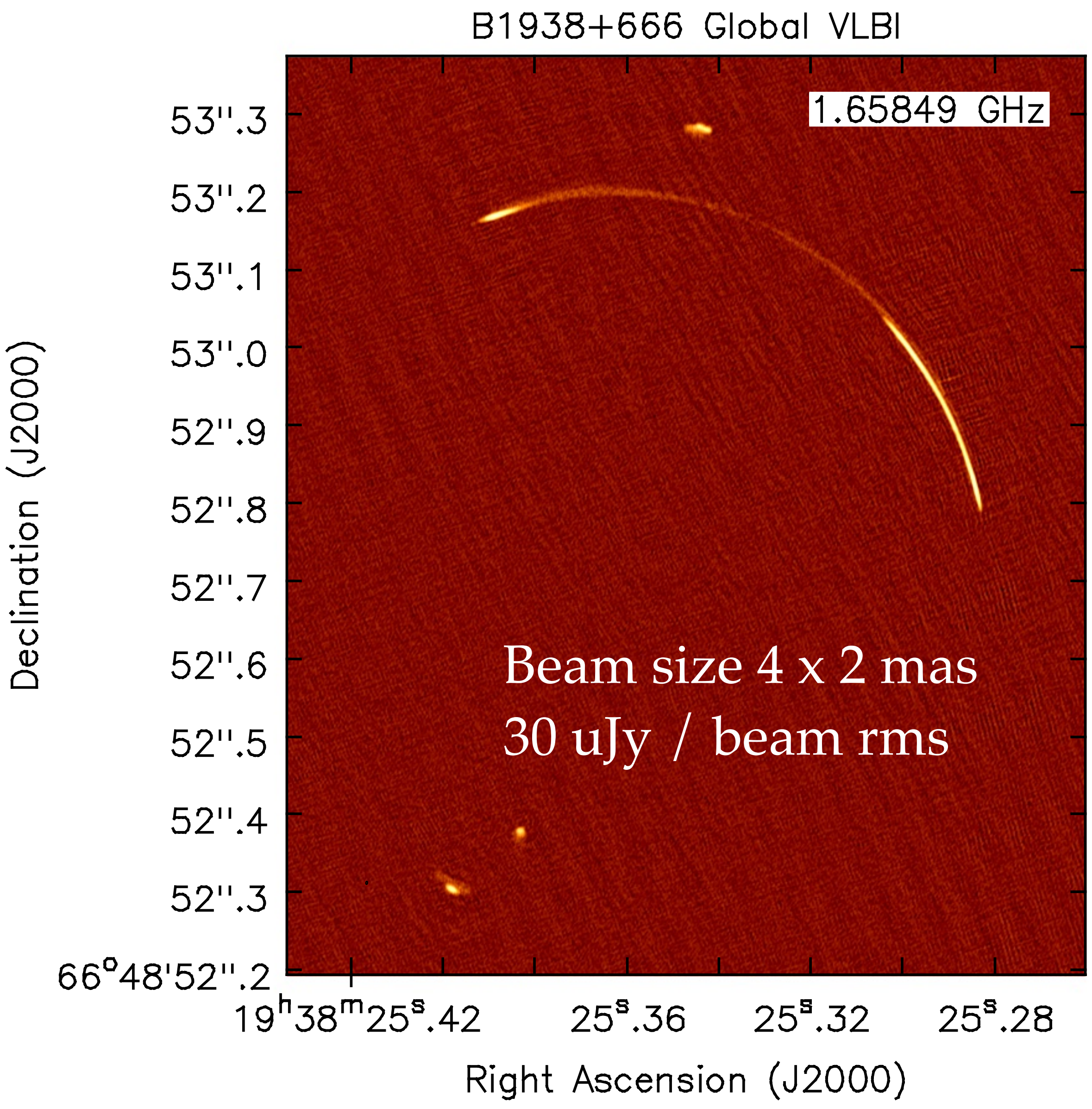

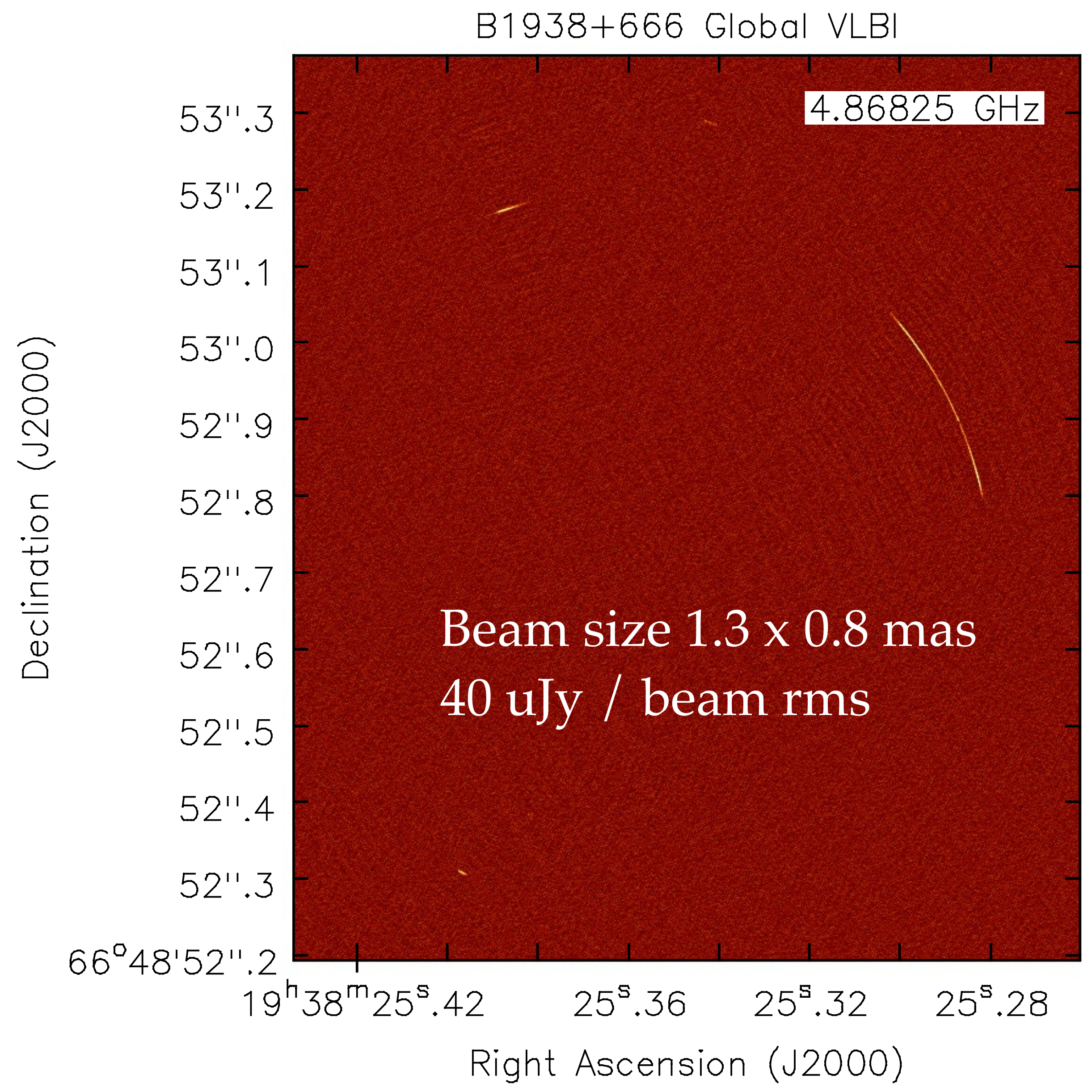

The quest for the smallest (sub)structure

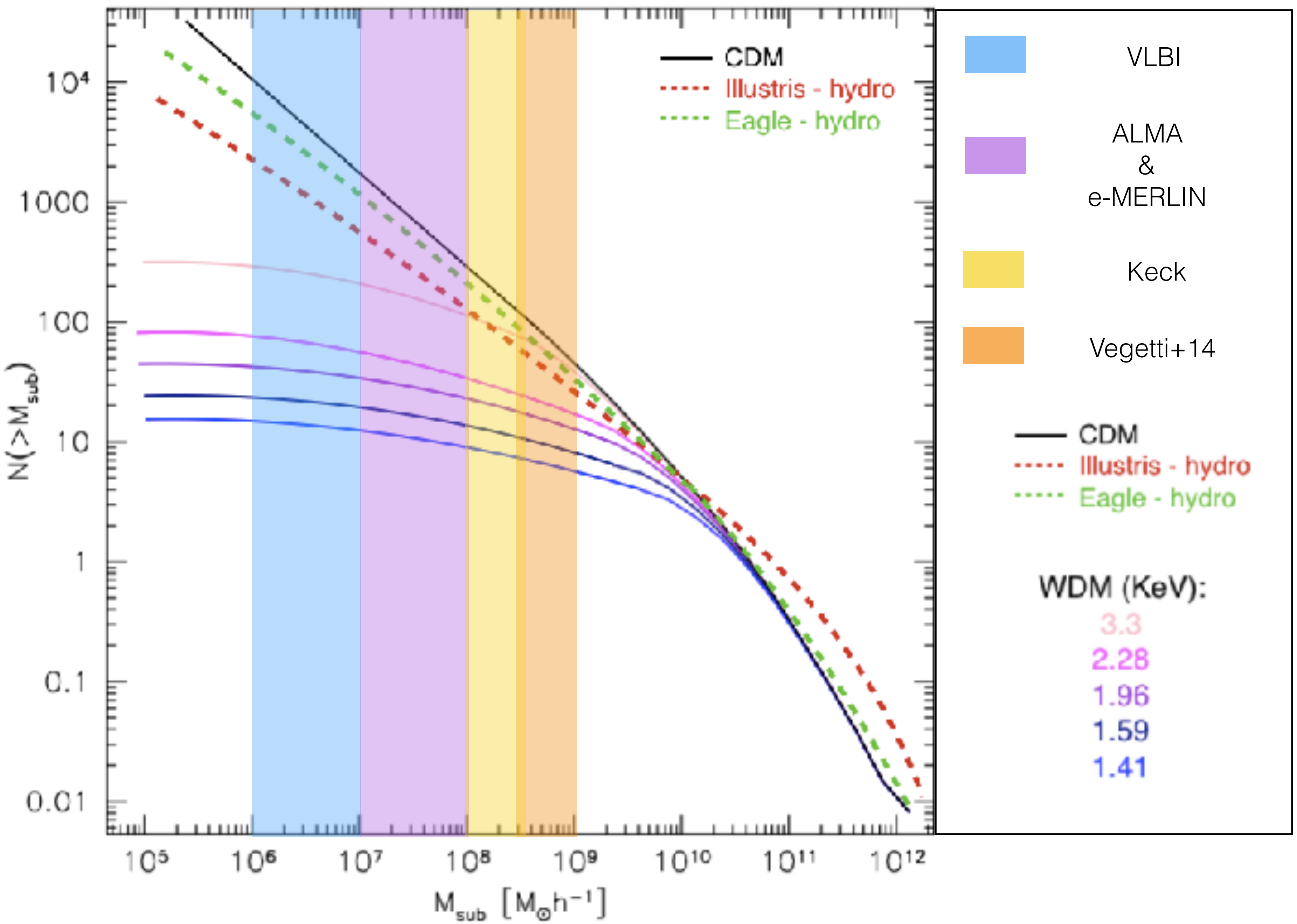

In summary

- Gravitational lensing provides a key probe on the nature of dark matter
- Using state-of-the-art lens modelling codes together with a wide range of observations we are now able to probe the the halo mass function from $10^9 M_{sun}$ all the way down to $10^6 M_{sun}$ and its evolution across cosmic time
- Interferometers are the key ingredient to detect the lowest substructure but require new dedicated lens modelling tools
- Structures along the LOS represent a significant contribution and provide a clean probe on the properties of dark matter
- Using high-resolution hydrodynamical simulations we can make consistent predictions for the (sub)structure mass function and investigate the degeneracies

Comparison with image-plane

Swinbank et al. 2015

The compact components are seen to vary between the two methods

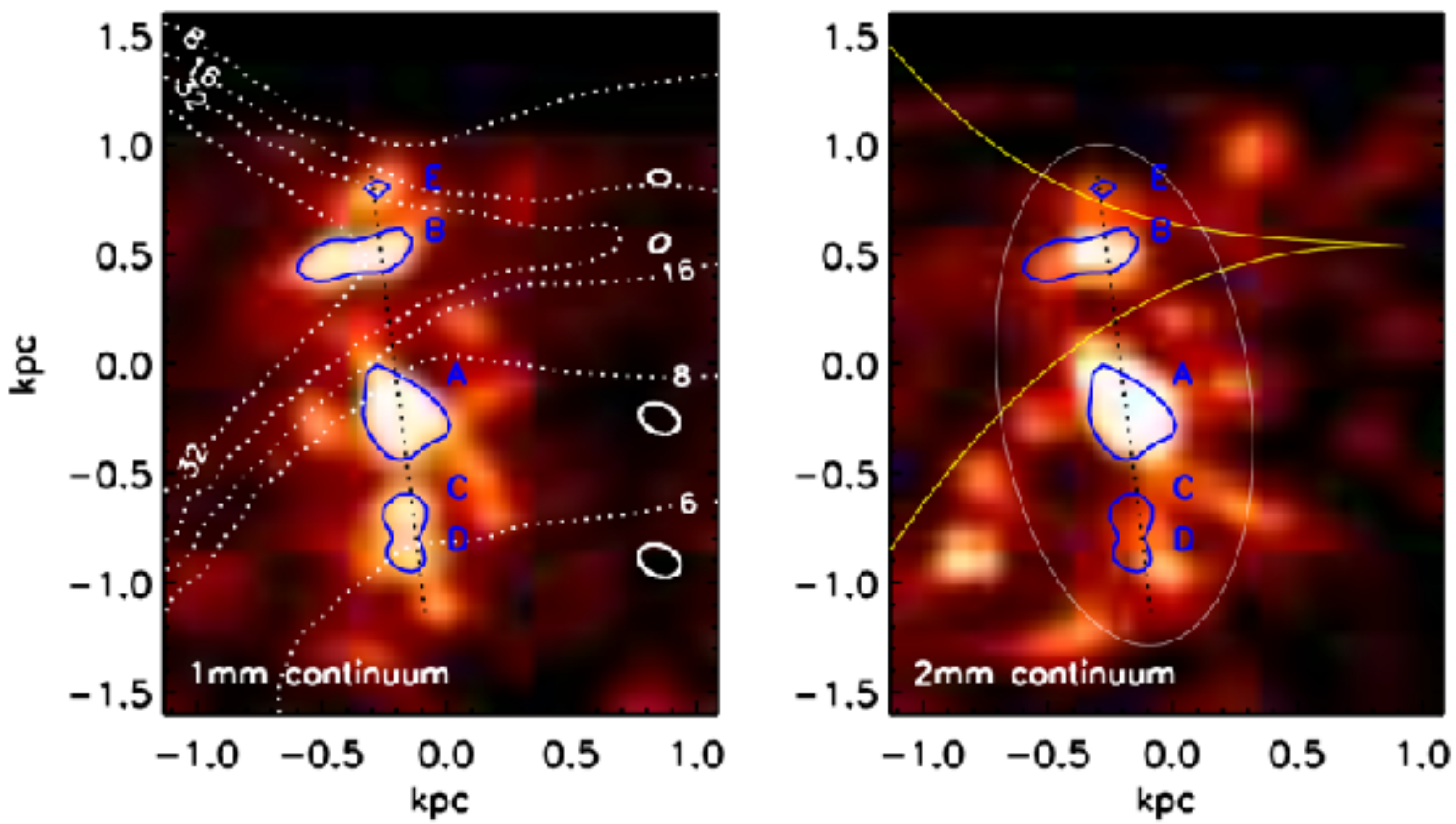

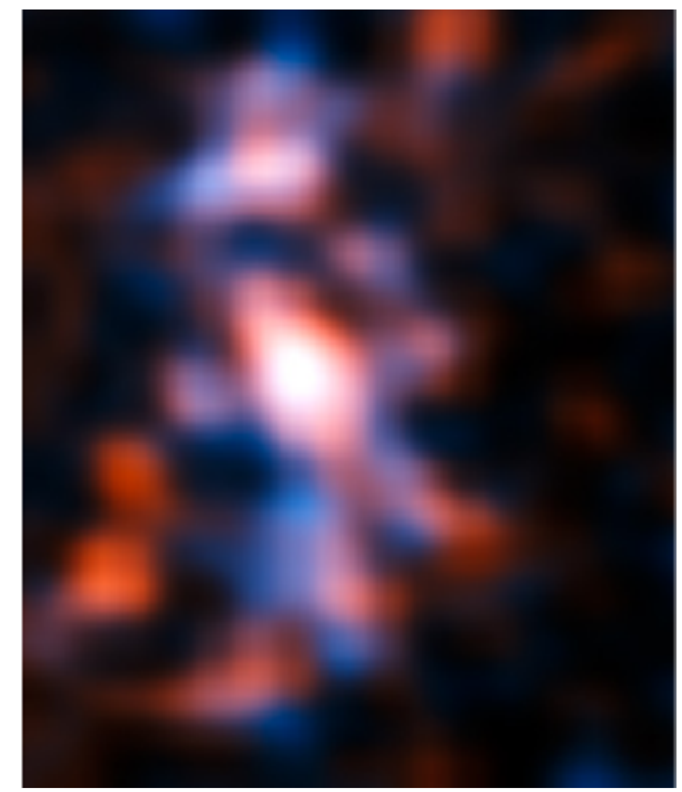

The compact structure varies significantly even within the individual image-plane analyses of the 1, 1.3 and 2 mm continuum data

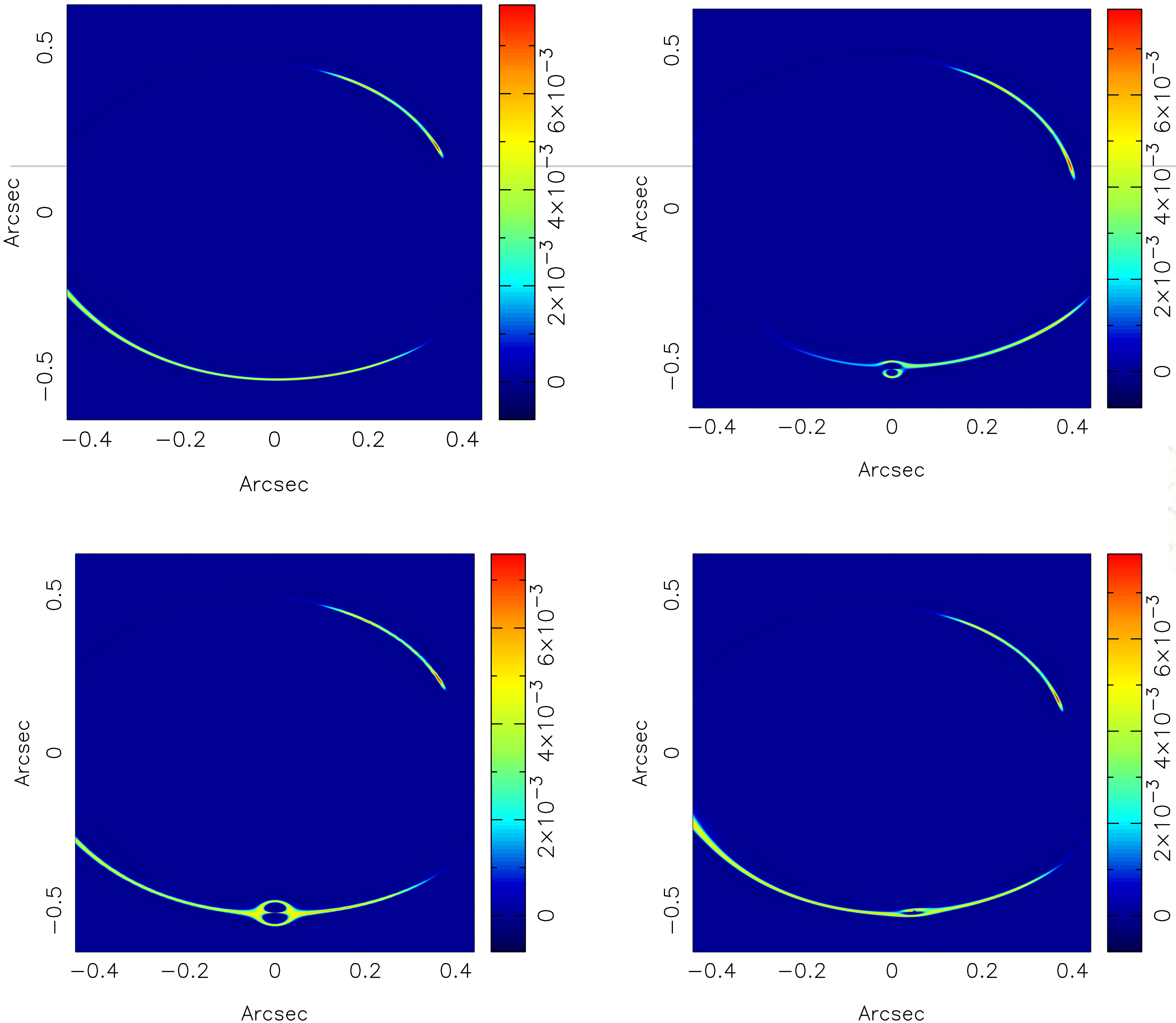

$$\xi_E = 4\pi \left(\frac{\sigma_{1D}}{c}\right)^2 \frac{D_{ds}}{D_s}$$